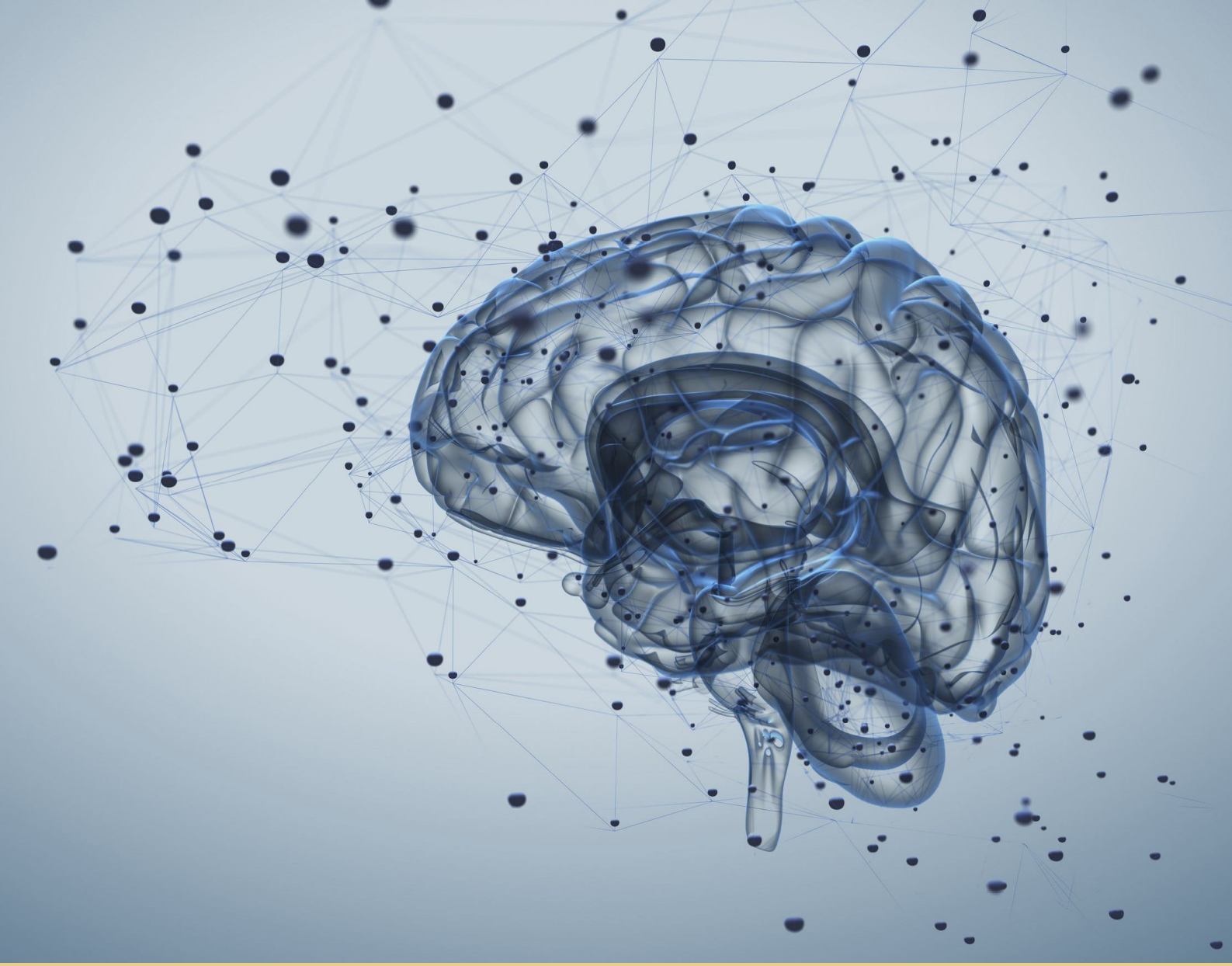

João André Figueiredo Pereira

REAL TIME fMRI NEUROFEEDBACK BASED ON INTERHEMISPHIRIC FUNCTIONAL CONNECTIVITY: A MOTOR IMAGERY PARADIGM

Dissertation presented to the University of Coimbra to obtain a degree of Master in Biomedical Engineering.

Coimbra, 2017

· U C ·

UNIVERSIDADE DE COIMBRA

• U C •

FCTUC FACULDADE DE CIÊNCIAS
E TECNOLOGIA
UNIVERSIDADE DE COIMBRA

João André Figueiredo Pereira

Real time fMRI Neurofeedback based on interhemispheric functional connectivity: a motor imagery paradigm

Dissertation presented to the University of Coimbra to obtain a degree of Master in Biomedical Engineering

Supervisors:

Prof. Dr. Miguel Castelo-Branco (IBILI, Faculty of Medicine, University of Coimbra)
Dr.Bruno Direito (IBILI, Faculty of Medicine, University of Coimbra)

Cover Image available at:

http://www.istockphoto.com/no/photo/brain-activity-gm497749034-79292021?st=_p_brain

Coimbra, 2017

This work was developed in collaboration with:

Institute for Biomedical Imaging and Life Sciences, Faculty of Medicine, University of Coimbra

Faculty of Medicine of the University of Coimbra

Dedicatória

Aos meus pais e avós,
pelo que sei que isto significa para vós.

Agradecimentos

Todo este trabalho não teria sido realizado sem a ajuda de um grupo de pessoas, às quais tenho de agradecer por terem tido um contributo especial.

Primeiro, um agradecimento ao Professor Miguel Castelo-Branco pela oportunidade que me proporcionou ao integrar um projeto desta envergadura no IBILI e pela incrível capacidade de, embora estar envolvido em dezenas de projetos, não precisar de mais que 2 segundos para se lembrar de todos os pormenores do meu e oferecer soluções para os problemas que foram aparecendo.

De seguida, um especial agradecimento ao Bruno Direito, por todo o acompanhamento e mentoria feita ao longo deste projeto, por toda a ajuda e conselhos que fizeram deste último ano uma experiência de aprendizagem total, em termos científicos e não só.

A todo o grupo *Calções e T-shirt*, em particular ao pessoal da *Sala de Cálculo* e às pessoas dos almoços diários. Vocês são tão genuinamente boas pessoas, que isso fez com que por vezes tivesse de ser relembrado do quão brilhante vocês são naquilo que fazem. É um dos melhores elogios que posso dar. Muito obrigado pelo ambiente e… *Eu queria escrever mais mas são 12h29 e não sei porquê...estou com uma fome dos diabos, vou almoçar e já venho!*

Um especial agradecimento à Sónia e ao Carlos Ferreira da Ressonância, por toda a ajuda e por terem aturado todas as minhas peripécias, merecem todos e quaisquer lanches. Um obrigado também à Daniela Pereira por toda a ajuda, incluindo na confirmação da seleção das áreas cerebrais online.

Um agradecimento a todos os participantes na minha experiência, o vosso contributo foi fulcral. E um especial agradecimento ao João Duarte por toda a disponibilidade e abertura para efetuar as experiências piloto.

E um agradecimento final, mas do tamanho do mundo a ti, Adriana, que estiveste ao meu lado todos os dias desde os últimos seis anos, pelo apoio e carinho constante que me faz tornar, a cada dia que passa, uma melhor pessoa. Tu, de facto *"just get me like i've never been gotten before".*

Resumo

A técnica de imagem usando ressonância magnética funcional (IRMf) é uma abordagem eficaz para medir a função cerebral, uma vez que pode medir o sinal dependente do nível de oxigénio no sangue (BOLD), uma medida indireta da atividade neural. Recentes avanços permitiram o desenvolvimento de IRMf em tempo real (rt-fMRI), em que o sinal BOLD de uma (ou mais regiões) está disponível em tempo real. Neurofeedback (NF) é um tipo de biofeedback em que uma representação visual, auditiva ou outra de natureza cognitiva, da atividade cerebral medida (região específica de interesse - ROI - ou correlação de dois substratos neurais de uma rede funcional) é apresentada ao participante para facilitar a auto-regulação desses correlatos neurais. Há evidências crescentes de que há mudanças patológicas na interação entre regiões cerebrais associadas a distúrbios psiquiátricos e neurológicos. Uma experiência rt-fMRI-NF pode permitir a manipulação na interação funcional entre regiões, representando assim uma maneira de estudar a relação entre comportamento e auto-regulação de medidas de conectividade. NF baseado em conectividade foi previamente sugerido como uma abordagem promissora, possivelmente fornecendo um melhor indicador de um aumento na dificuldade da tarefa, bem como uma ferramenta valiosa para melhorar a aprendizagem e neuroreabilitação. Este projeto visa projetar e testar um protocolo que permita aos participantes auto-regular a conectividade funcional em tempo real, calculada com uma Correlação de Pearson com janelas deslizantes, entre regiões que se sobrepõem durante performance motora (MP) e imaginação motora (MI), como o córtex premotor bilateral (PMC). Para este fim, os participantes são encorajados a adaptar tarefas de imaginação motora. A nossa hipótese é baseada na noção de que controlo de aprendizagem sobre substratos neuronais específicos (ou interações entre regiões), modifica comportamentos específicos, função cerebral e neuro plasticidade, podendo representar uma estratégia terapêutica para distúrbios relacionados à conectividade. Os resultados mostram que os participantes foram capazes de modular conectividade inter-hemisférica obtendo representação visual do valor de correlação entre PMC bilateral como neurofeedback em tempo real. Isto suporta a ideia de que é possível criar uma aplicação terapêutica de treino motor em indivíduos com diminuição da conectividade inter-hemisférica, como doentes com que sofreram de AVC.

PALAVRAS-CHAVE: *fMRI, Neurofeedback baseado em conectividade, Conectividade Funcional*.

Abstract

Functional magnetic resonance imaging technique (fMRI) is an effective approach to measure brain function since it can measure blood oxygenation level-dependent (BOLD) signal, an indirect measure of neural activity. Recent advances allowed the development of real-time fMRI (rt-fMRI), in which the BOLD signal of one (or more regions) is available in real-time. Neurofeedback (NF) is a type of biofeedback in which a visual, auditory or cognitive representation of the measured neural activity (specific region of interest - ROI - or correlation of two neural substrates of a functional network is presented to the participant to facilitate self-regulation of the neural correlates. There is increasing evidence that there are pathological disturbances in the functional interaction between brain regions associated to psychiatric and neurological disorders. A Real-time Functional Magnetic Resonance Imaging Neurofeedback (rt-fMRI-NF) experiment might enable the manipulation of interactions between regions, and thus represents a way of investigating the relationship between behavior and self-regulation of connectivity measures. Connectivity-based NF has previously been confirmed as a suitable approach for neurofeedback implementation and possibly a valuable tool to enhance motor learning and rehabilitation. This project aims to design and test a framework that enables the participants to self-regulate the functional connectivity, calculated with a windowed Pearson Correlation, between regions that overlap during motor performance (MP) and motor imagery (MI) such as bilateral premotor cortex (PMC) in real time. To this end, participants are encouraged to use a adaptive motor imagery task. Our hypothesis is based on the notion of learning control over specific neural substrates (or interactions between regions) changes specific behaviors, brain function and neuroplasticity, and may represent a therapeutic strategy for connectivity-related disorders. The results show that the participants were able to modulate interhemispheric connectivity while getting visual representation of the value of correlation between bilateral PMC as real-time neurofeedback. This supports the idea that it is possible the design a motor training as a therapeutical application in subjects with decreased interhemispheric connectivity such as stroke patients.

KEYWORDS: *fMRI, Connectivity-based Neurofeedback, Functional Connectivity.*

List of Acronyms

AC Anterior Comissure
ACPC Anterior Comissure Posterior Comissure
ALS Amyotrophyc Lateral Sclerosis

BA4 Broadmann Area 4
BA6 Broadmann Area 6
BCI Brain-Computer Interfaces
BOLD Blood Oxygenation Level-Dependent
BV BrainVoyager

CBF Cerebral Blood Flow
$CMRO_2$ Cerebral Metabolic Rate of Oxygen
CNS Central Nervous System

DCM Dynamic Causal Modeling
dHb Deoxyhemoglobin
dlPFC Dorsolateral Prefrontal Cortex

EEG Electroencephalography

FA Flip Angle
fMRI Functional Magnetic Resonance Imaging Technique
fNIRS Functional Near-Infrared Spectroscopy
FOV Field of View

GLM General Linear Model

Ha Alternative hypothesis
Hb Hemoglobine
H0 Null Hypothesis
HRF Hemodynamic Response Function
lFG Inferior Frontal Gyrus

lM1 Left Primary Motor Cortex
lPMC Left Premotor Cortex

M1 Primary Motor Area
MR Magnetic Resonance
ME Motor Execution
MI Motor Imagery
MIQ-3 Movement Imagery Questionnaire-3
MP Motor Performance
MPRAGE Magnetization-Prepared Rapid Acquisition Gradient Echo
MRI Magnetic Resonance Imaging

NF Neurofeedback

PC Posterior Comissure
PMC Premotor Cortex
PMd Dorsolateral Premotor Cortex
PMd-lM1 Dorsal Premotor to Left Primary Motor Cortex
PMdr Rostral Portion of the Dorsal PMC
PMv Ventrolateral Premotor Cortex

RFX Random Effects
rMI Right Primary Motor Cortex
ROI Region of Interest
ROIs Regions of Interest
rPMC Rght Premotor Cortex
rPMD Rght Dorsal Premotor Cortex
rt-fMRI-NF Real-time Functional Magnetic Resonance Imaging Neurofeedback.

SMA Supplementary Motor Area
SMAr Right Supplementary Motor Area
SNR Signal to Noise Ratio
STG Superior Temporal Gyrus

TAL Talairach Space
TBV Turbo-BrainVoyager
TE Echo Time
TMS Transcranial Magnetic Stimulation
TR Repetition Time

vmPFC Ventromedial Prefrontal Cortex

Table of Contents

List of Tables

List of Figures

List of Equations

Introduction

"The human brain has 100 billion neurons, each neuron connected to 10 thousand other neurons. Sitting on your shoulders is the most complicated object in the known universe."

Michio Kaku, 2014

One of the best ways to understand how the brain works and the connections that form neural networks even while performing simple tasks, is based on the functional magnetic resonance imaging (fMRI) technique. fMRI measures the blood oxygenation level dependent (BOLD) signal, an indirect measure of several biophysical and physiological sources, based on the body's natural magnetic properties, as in magnetic resonance imaging (MRI) technique. Based on these properties, it is possible to produce detailed images from the human brain as well as functional information from underlying processes occurring within (Sulzer et al., 2013).

BOLD signal and Real time fMRI

The fMRI is a noninvasive method with high spatial resolution able to do whole Brain coverage, an advantage over other non-invasive neuroimaging methods such as the electroencephalography (EEG) or functional near-infrared spectroscopy (fNIRS) (Sulzer et al., 2013). It measures changes in the amount of oxygenated blood, the BOLD signal. This signal represents an indirect measurement of neuronal activity since there is increasing evidence of a coupling between the BOLD signal and the electrical activity of neurons (Sitaram et al., 2011).

Real time fMRI (rt-fMRI) allows simultaneous measurement and observation of the neural activity of a subject in real-time, while performing a task. Online image reconstruction and statistical analysis of reconstructed images happens within a single repetition time (TR), usually between 1.5-2 seconds, allowing the observation of the activity of the brain while the measurement is occurring (Sitaram et al., 2011). This application led to new interactive experimental paradigms to be created, making fMRI a better and more flexible tool for functional/neurological studies (Sulzer et al., 2013).

The study of connectivity based on fMRI data: from functional segregation to functional integration

Over the last two decades, neuroimaging has become a crucial technique in neuroscience (Friston, 2011). From a historical perspective, imaging neuroscience has established as the main goal the study of functional segregation (cortical regions specialized for a specific function, anatomically clustered within the cortex). Recently, a trend emerged emphasizing the relevance of studying functional integration, i.e. the connections between segregated areas. This reflects a shift from functional segregation to functional integration studies, and represents an increased interest in the functional integration of anatomically separated brain areas and their connectivity (Friston, 2011). When it comes to connectivity, there are two different concepts with different analytic approaches and from which conceptually information is inferred: functional and effective connectivity (Friston, 2011).

On the one hand, effective connectivity analysis can be associated with studying hypotheses regarding how the brain works and the influence of one neural system on another neural system. On the other hand, functional connectivity analysis addresses a more pragmatic issue of differentiating conditions or subjects by measuring distributed brain activity in two or more areas using covariances and correlations between them without direct inference on direction of influence (Friston, 2011).

Functional connectivity, in neuroscience imaging is defined as statistical dependency between remote or distinct neurological events. It is treated as an observable phenomenon that can be quantified with measures of statistical dependencies, such as correlations, coherence, or transfer entropy (Gerstein and Perkel, 1969). In fMRI experiments it is assumed that correlation of low frequency fluctuation is a manifestation of functional connectivity of the brain, since these result from fluctuations in blood oxygenation or flow, i.e, the BOLD signal (Biswal et al., 1995).

rt-fMRI Neurofeedback

Neurofeedback (NF) is a technique that allows a subject to have access to real time information of its brain activity designed to train the individual to self-modulate a specific brain region, combination of regions, or connectivity between regions. Several neurological disorders present impaired brain activation patterns, and neurofeedback-based training may represent a therapeutical alternative. NF could have the potential to help a subject on a long-term basis with slim risk of harm (Coben, Linden, and Myers, 2010).

The motor/premotor cortex/network as a specific target for BCI applications and neurofeedback training

Studies of motor integration imply the understanding of the conversion of sensory inputs into an adequate effective motor commands determined within the central nervous system (CNS).

Motor imagery is defined by Decety (1996) as a dynamic state in which the subject mentally simulates a particular action so that he can feel himself performing the imagined action. It belongs in to same category of brain processes as the ones which are involved in motor performance, but requires an additional inhibitory process to prevent the imagined movement from actually happening, in prefrontal and dorsolateral frontal cortex (Jeannerod, 1994), (Piokenhain, 1984).

With the evolution of brain-computer interfaces (BCI), it is now possible to create controlled environments where a subject interacts with a computational model providing a way to study motor control, planning and even learning (Wolpert and Ghahramani, 2000). The motor network has been extensively. In particular, several BCI studies focused on rehabilitation training using real, virtual, and augmented approaches, exploiting brain signals generated from healthy people and patients along with decoded kinematic parameters (Abdulkader, Atia, and Mostafa, 2015).

Connectivity and the motor processing network

Every motor action is a dynamic result of the operation of numerous brain areas working in different aspects from motion planning to actual performance. This integration may be described by effective connectivity models which may help us understand how different motor areas work to promote motor activity (Grefkes et al., 2008).

When a person performs a task that requires communication between the two cerebral hemispheres (in areas such as the visual cortex for visual perception or motor cortex for simple actions such as tying shoelaces) there is an underlying common activity between both hemispheres that can be measured by connectivity metrics (Stephan et al., 2007).

1.1. Motivation and relevance

There are numerous diseases involving neuronal processes in which there is a loss or destabilization in the interhemispheric connectivity of a subject such as: Parkinson's, Amyotrophic lateral sclerosis (ALS), Tourette's, Autism Spectrum Disorders, major depressive disorder and specifically when speaking about motor cortex, stroke (New et al., 2015).

For that purpose, this project aims at the design and test a neurofeedback framework that enables the participants to self-regulate the interhemispheric connectivity between bilateral premotor cortices (PMC).

Accounting for this project's main purpose, we propose a novel motor imagery task and evaluate networks involved. Thus, our hypothesis is based on the fact that these regions may represent a suitable neurofeedback target for connectivity based NF.

1.2. Main Contributions

The main contributions of this work are:

- The first use of PMC for functional connectivity-based, rt-fMRI-NF experiment;
- Optimization of an imagery paradigm allowing to use the BOLD response for up-regulation of the connectivity of bilateral PMC by means of correlation measures;
- Functional connectivity-based rt-fMRI-NF with the implementation of both up and down-regulation conditions (the former showing larger success).

1.3. Research Question

Is it possible to modulate interhemispheric connectivity between bilateral PMC in a rt-fMRI-NF experiment based on a motor imagery paradigm?

What is the best approach to optimize correlation modulation using such a NF paradigm?

fMRI and functional connectivity: from BOLD to functional connectivity feedback

2.1. BOLD signal

Magnetism is a property of matter, generated by its electrically charged components, such as protons or electrons. Atoms and molecules have electron orbitals that, depending on the number of electrons being even or odd, either cancel each other's magnetic properties or create a magnetic field. The ability of a material becoming magnetized when in presence of an external magnetic field and the extension of which is called *magnetic susceptibility* (Ravenel, 2003).

Magnetic Resonance (MR) signals are extremely significant for neuroscience studies due to the fact that it is possible to measure T2* - the observed transverse magnetization caused by natural interactions at the atomic or molecular levels after a radiofrequency pulse - with high spatial resolution in “whole brain” scans superimposing small gradients to the main B0 magnetic field. The mechanism that allows to link neural activity and measurable T2* is called the BOLD contrast (Logothetis and Wandell, 2004).

The hemodynamic BOLD signal is interpreted as an indirect measure of brain. It does not correlate perfectly with action potentials, and does instead measures a combination of continuous membrane potentials and action potentials (Arthurs and Boniface, 2002).

The T2* parameter alteration in the BOLD signal mechanisms is explained by changes in the relative concentration of oxygenated and deoxygenated blood. Deoxyhemoglobin (dHb) is paramagnetic and has a strong contribution to the MR signal. In the presence of deoxygenated blood there is an increased concentration of dHB and therefore an increased magnetic susceptibility and consequently the T2* decreases. This variation allows the generation of contrasts (Logothetis and Wandell, 2004).

BOLD contrast is determined by the balance of oxygenated and deoxygenated blood flow required in a certain brain region based on increased or decreased neuronal activity (Stephan et al., 2007). Areas more intensely activated require a higher concentration of oxygen and nutrients in the blood, increasing the BOLD signal in that particular region. The time course of the human BOLD

response to a momentaneous stimulus ("impulse") has been previously studied and is known as hemodynamic response function (HRF) (Siero, Bhogal, and Jansma, 2013).

HRF typical response consists of mainly 3 parts, represented in the **Figure 1**. The first is a small, short-lived negative deflection of the BOLD signal during the first 1 to 2 seconds called the initial dip, thought to indicate an increase in cerebral metabolic rate of oxygen ($CMRO_2$) before the cerebral blood flow (CBF) response. The second part is related to a larger signal increase caused by a large CBF increase that peaks around 3 to 6 seconds, followed by a signal decrease. Finally, there is a subsequent post stimulus undershoot before returning to baseline after 12 to 30 seconds (Siero, Bhogal, and Jansma, 2013).

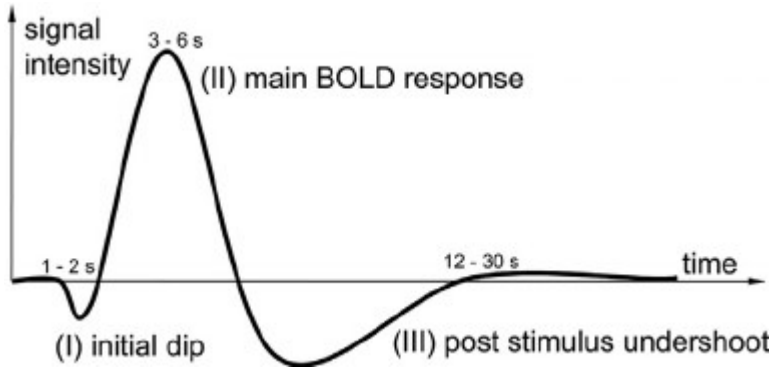

Figure 1. Typical BOLD hemodynamic response function. The shape can vary depending on the stimulus conditions, cortical area, and the biology of the local vasculature (Siero, Bhogal, and Jansma, 2013).

2.2. fMRI protocol

One of the main applications of fMRI is to locate the neural correlates in sensory, motor or cognitive processes. The term "brain mapping" is commonly used to describe this goal of relating specific operations and tasks to specific areas and networks in the brain. Another major goal of fMRI studies is the detailed characterization of a response profile across experimental conditions given regions-of-interest (ROI). fMRI experimental protocols are mostly based on two types of designs: *block design* and *event related design* (Mulert and Shenton, 2014).

2.2.1. Block design protocol

Block design was the first type of experimental paradigm to be used in fMRI research. It is still the most commonly used experimental paradigm in fMRI studies.

Let us consider a paradigm with two conditions: baseline and activation. The temporal structure would consist of several discrete epochs usually ranging from 16 to 60 seconds, alternating between conditions, **Figure 2**.

The idea is to analyze the BOLD signal fluctuation during the experiments, and use a statistical framework to associate the variation of the BOLD signal to the different conditions.

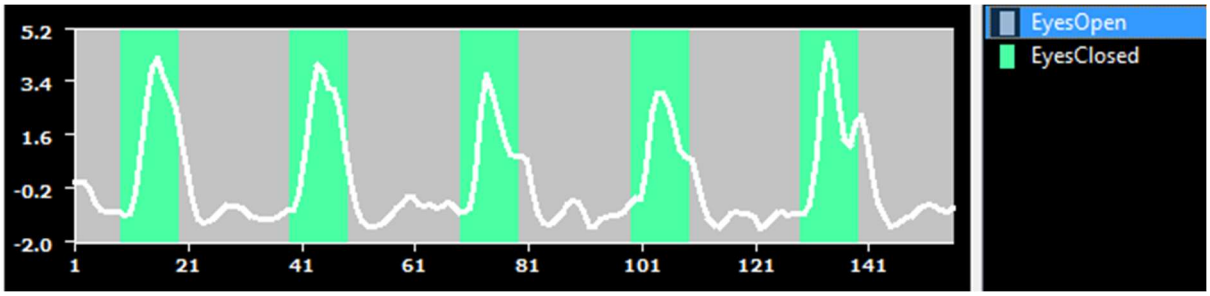

Figure 2. Block design fMRI with the BOLD response corresponding to two different conditions ("Eyes Open", "Eyes Closed") in a block design paradigm using BrainVoyager software.

The block design is considered most adequate for many types of experiments. It is powerful and flexible, allowing to study as many conditions as the researchers intend and adequate block duration for the different complexity tasks used. It also has a higher statistical power and allows a straightforward analysis (Barron, Garvert, and Behrens, 2016). However, the block design is susceptible to confounds such as strategy effects, fatigue and repetition suppression, which may induce variability of the BOLD signal across the epochs of interest (Barron, Garvert, and Behrens, 2016).

The alternative design, event-related, aims to associate brain processes with discrete and singular events, allows greater randomization but with a lower signal-to-noise (SNR) ratio that, in order to compensate, could lead to a longer session for the subject (Josephs and Henson, 1999).

2.3. BOLD and neurofeedback

2.3.1. Neurofeedback

Neurofeedback is a specific type of biofeedback in which neural activity is measured and presented to the participant in real time through a visual, auditory or another representation in order to

facilitate self-regulation of their own neural substrates that underlies a specific behavior or pathology (Sitaram et al., 2017).

2.3.2. BOLD signal as neurofeedback in fMRI

With the development of rt-fMRI, first implemented by Cox, Jesmanowicz, and Hyde (1995), it became possible to process online the functional images from the MRI scanner. This online processing paved the way for a new type of experiment in which stimuli can be adjusted as a function of the brain activation of the participant, and is known as NF (Weiskopf, 2012).

Since the first experiment (Weiskopf et al., 2004), many studies have been reported, exploiting higher resolutions of rt-fMRI, where healthy volunteers can learn to self-regulate the local BOLD response with the help of rt-fMRI neurofeedback (Weiskopf, 2012).

For potential confirmation of the possible applications in clinical neuroscience, specific behavioral effects during the self-regulation and training effects maybe observed (Weiskopf, 2012).

Recently there have been developments in neurofeedback experiments that use the brain activation of more than one region, feeding back the information concerning the interaction between these areas - their functional and effective connectivity. This topic will be detailed in the Literature Review chapter.

Literature review: a motor imagery paradigm

3.1. Rationale / Overview

Recently there has been a growing interest in connectivity studies among distinct brain areas, since deficient or poorly regulated functional connectivity patterns have been linked with disorders such as autism (Minshew and Keller, 2010), motor dysfunction (Poston and Eidelberg, 2012), schizophrenia (Stephan, Baldeweg, and Friston, 2006) among others. This implies a shift from the segregation paradigm based on univariate activation, single or a small local agglomerate of voxels, to connectivity paradigms that emphasize the bivariate or multivariate covariance or synchronization of segregated brain areas, allowing the study of systems or networks (Bullmore, 2012).

3.1.1. fMRI connectivity studies

The first fMRI studies dedicated to the activation patterns in the human brain had their main focus in measuring spontaneous activation patterns of anatomically separated brain areas, reflecting the level of functional communication between these regions while in resting state or even in specific task performance (van den Heuvel and Hulshoff Pol, 2010). Concerning the motor cortex, Biswal et al. (1995) first revealed, in a bilateral finger tapping task, the existence of low frequency fluctuations in fMRI signal intensity in sensorimotor cortex regions that had a high degree of temporal correlation and concluded that the primary motor area (M1) and supplementary motor area (SMA) are involved in motor execution, **Figure 3**.

Figure 3. Low frequency fluctuations reported by Biswal et al. (1995), with a and b being the right and left motor cortex, c the SMA and d the paracentral lobule. Red corresponds to positive correlation, and yellow corresponds to negative.

Sun et al. (2007) studied the effect in functional connectivity of cortical networks with the learning of new motor skills using task-specific low frequency coherence analysis of the data. The authors concluded a greater intra and inter hemispheric coupling within the cortical motor network, the sensorimotor cortex, PMC and SMA in early stages of learning a motor skill and as well as a higher connectivity between frontal and motor regions. Sun et al. (2007) results demonstrate the modulation of functional connectivity of motor networks with learning and practice of motor skills and its relation to increase of difficulty tasks.

3.2. Evidence of connectivity changes based on NF training

3.2.1. rt-fMRI Activation based – NF

In NF training based on rt-fMRI, changes in activation patterns in specific brain areas responsible for cognition (Weiskopf, Scharnowski, et al., 2004), behavior (Rota et al., 2009), and emotion (Caria et al., 2010) have been reported. However, these are not the focus of this thesis. For a review see the work of Emmert et al. (2016).

3.2.2. Connectivity-based fMRI-NF

3.2.2.1. Effective connectivity based "near real time fMRI-NF"

In order to get a more robust knowledge of the communication pathways during a visual-spatial attention paradigm, Koush et al. (2013) tested the feasibility of using effective connectivity measures within a neurofeedback setup by presenting near real-time dynamic causal modeling (DCM) as a calculation of feedback based on connectivity between brain areas rather than activity in a single brain region. DCM is a hypothesis driven approach that requires the formulation of a specific network of connectivity between ROIs and of experimental factors that modulate these connections. In this experiment, participants were asked to voluntarily modulate connectivity either between left visual cortex and left parietal cortex or between right visual cortex and right parietal cortex.

Each neurofeedback run, optimized to 90 points sliding window in order to achieve a faster and stable Bayesian model comparison, was followed by a minute block of resting state, during which the feedback signal was computed for it to be presented visually to the participant. Koush et al. (2013)

concluded, in this proof-of-concept, the feasibility of effective connectivity as neurofeedback in near real time fMRI since feedback was voluntarily controlled by the participants.

For real-time data analysis, the connectivity-based feedback signal needs to be computed within a relatively short time window, so a method providing robust estimates with a few data points may have the priority in this context, comparing to more robust statistical models such as DCM (Zilverstand et al., 2014).

3.2.2.2. Functional connectivity-based rt-fMRI-NF

Recently, there have been further technological developments in order to facilitate functional connectivity studies and/or spatio-temporal patterns analysis of brain activity as neurofeedback in real-time fMRI studies. A systematic comparison regarding the sensitivity of different connectivity methods showed that correlation presents good sensitivity, performing among the top four of the twelve investigated methods (Smith et al., 2011).

Ruiz et al. (2014) performed the first study aiming self-modulation of functional connectivity of two distinct brain regions with rt-fMRI-NF experiment. In this study, a group of healthy participants were trained to increase the functional connectivity between fronto-temporal cortex, more specifically inferior frontal gyrus (IFG) and superior temporal gyrus (STG), during self-regulation blocks with visual feedback of the correlation coefficient. The feedback was calculated with a sliding window correlation coefficient considering current and past time points. Ruiz et al. (2014) results show that participants were able to learn how to self-regulate their functional connectivity between IFG and STG after a few sessions of training and that there were behavioral modifications induced by the NF-training in a semantic priming task.

More recently, Spetter et al. (2017) developed a functional connectivity-based rt-fMRI-NF experiment, in which subjects were proposed to up-regulate functional connectivity between the dorsolateral prefrontal cortex (dlPFC) and ventromedial prefrontal cortex (vmPFC), considered to be important areas in the executive control and reward processing. Spetter et al. (2017) trained eight male subjects with overweight or obesity in a four-day, three training runs a day, rt-fMRI neurofeedback protocol with six up-regulation and six passive viewing trials. Results show that the participants successfully learned to increase functional connectivity between the selected areas, indicating that

overweight and obese participants can modulate connectivity between brain areas that regulate control of appetite, being therefore a possible technique for achieving weight loss.

Recently, a clinical trial has been completed by Benjamin Becker (2017), in order to evaluate, in healthy subjects, whether real-time fMRI neurofeedback training can enable individuals to gain volitional control over their fronto-limbic connectivity, important to emotional perception and its regulation. According to the authors, the hypothesis is that subjects that receive real feedback develop a more controlled emotional response comparing to the subjects that received sham neurofeedback, over the course of the three day neurofeedback training [1].

3.3. Motor cortex

3.3.1. Anatomical references and functions

With the evolution of anatomical and functional imaging techniques, first in non-human primates and later in humans, it was possible to again insight into the complexity of the cortical motor organization (Rizzolatti, Luppino, and Matelli, 1998).

The idea that each parietal area is involved in processing particular aspects of the sensory information and its analysis is corroborated by the multiplicity of areas with distinct anatomical and functional properties that constitute the posterior parietal lobe (Rizzolatti, Luppino, and Matelli, 1998).

The motor cortex is the agranular sector of the frontal lobe that occupies its caudal part and is formed by a mosaic of distinct areas, anatomically and functionally. Brodmann (1909) subdivided the motor cortex into two regions: the primary motor area (M1) in the area 4 (BA4) and the non-primary or premotor cortex area 6 (BA6).

Matsumoto et al., (2007) used histochemical and cytoarchitectural methods to further divide the non-primary motor cortex (BA6) in three areas: the medial premotor cortex, the dorsolateral premotor cortex (PMd) and the ventrolateral premotor cortex (PMv). Each of three distinct areas that make up the non-primary motor have an anatomical and functional subdivision in rostral and caudal (Matsumoto et al., 2007).

The caudal portion of the medial premotor cortex has substantial projections to M1 and to the spinal cord. The rostral parts of the medial premotor cortex are more interconnected with the prefrontal cortex (PFC) than M1 (Geyer et al., 2000), (Matelli et al., 2004).

3.3.2. Motor performance

Grefkes et al. (2008) established a statistical model (based on DCM) considering the various brain regions involved in movement preparation and execution in order to better understand the mechanisms underlying motor function, **Figure 4**. The authors found an intrinsic intra and interhemispheric balance of excitatory and inhibitory coupling in motor areas, using uni- and bimanual movements as tasks. The authors selected as ROIs the primary motor cortex (M1), premotor cortex (PMC) and supplementary motor area (SMA). The results suggest that in unimanual movements there is a suppression mechanism of the motor activation of the resting hand that targets M1 neural activity with negative coupling parameters. In terms of bimanual in-phase movements, Grefkes et al. (2008) reported an induced intra and interhemispheric effective connectivity in both hemispheres.

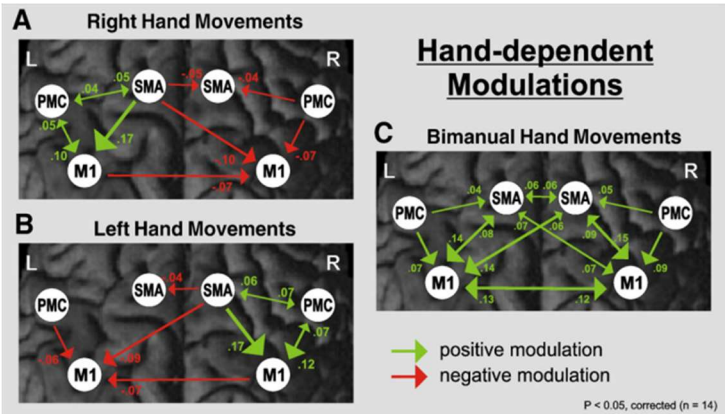

Figure 4. Results reported by Grefkes et al. (2008) reflect an enhanced connectivity towards contralateral primary cortex and neural coupling towards ipsilateral motor areas reduced during unimanual movements (A and B) and also symmetric facilitationl.

Liuzzi et al. (2011) studied the effective connectivity in uncoupled and coupled bimanual movement in brain regions such as SMA and PMC. The authors concluded that there is an increase of connectivity in right parietal areas, dorsal PMC (PMd) and prefrontal regions in the opposite hemisphere in uncoupled movements. It was also reported that strict time modulation of right premotor cortex to left primary motor cortex (rPMC-lM1) connectivity is essential for independent high frequency

use of both hands in contrast with coupled movements. Besides, there is an active involvement of right dorsal premotor (rPMd) in stabilization of anti-phase movements.

It was also noted the importance of timing of facilitation or successful anti-phase movements, meaning that early and strong facilitation was associated with better performance in bimanual anti-phase movements, whereas delayed facilitation was found in subjects with poor anti-phase stability.

Patterns of bimanual coordination in which homologous muscles are activated at the same time are known to be more stable than those in which the muscles are engaged in an alternate fashion (Aramaki, Honda, and Sadato, 2006). Aramaki, Honda, and Sadato (2006) used fMRI in order to investigate the neural representation of the interhemispheric connectivity in motor areas during bimanual mirror movements, using auditory cues and a sequence of finger tapping tasks. The activation in the right primary motor cortex (rM1) was less prominent during mirror bimanual tasks than on unimanual left-handed movements. This only happened in the non-dominant side, since parallel movements did not cause such reduction and left primary motor cortex (lM1) showed no statistical difference activation across the unimanual right, bimanual mirror, and bimanual parallel conditions. The authors concluded that, during mirror movements, the movement parameters of homologous muscles are specified in the lM1 while the rM1 is suppressed transcallosally, suggesting that the non-dominant motor system give away part of the control of its hand to the dominant motor system via the uncrossed efferent pathway.

Dorsal premotor cortex (PMd) has been shown by Hoshi and Tanji (2007) to reflect movement parameters like direction, amplitude and speed of arm movements. Transcranial Magnetic Stimulation (TMS) and microstimulation experiments allowed the authors to conclude that PMd facilitates the initiation of arm movement. Neurons in PMd are essential in conditional motor tasks. This has been seen in experiments with monkeys having this particular region activated in response to a visual cue, showing its intention to do a certain movement, and linked to its movement selection (Hoshi and Tanji, 2007).

Ventral Premotor Cortex (PMv) involvement in planning and execution arm movements is also well documented. It is established that the vast majority of PMv neurons are selective for the direction of the movement planned in the visual space regardless of the subject posture and the trajectory and direction of the imaginary motion. These neurons are selected for the transformation of visual space

to motor space, using the details and parameters from the target into motor information (Hoshi and Tanji, 2007).

The medial PMC is also related with movement selection although this region is selective to motor actions planned due to an internal cue rather than an external one, i.e., motor sequences from memory. Lesions in monkeys that had its medial PMC removed involved loss of self-initiated movements, i.e., movements without any external cue (Purves et al., 2001).

3.3.3. Motor Imagery

Hanakawa et al. (2003) compared functional neuroanatomy of motor performance (MP) and motor imagery (MI) while performing a finger-tapping sequence and obtained a statistical parametric map of brain areas with a movement-predominant activity, imagery-predominant and with activation common to both imagery and performance.

TABLE 1. *Brain areas activated more during the movement tasks than the imagery tasks*

Cluster Size	Locations (Brodmann area), Functional Areas	*x*	*y*	*z*	*Z*-Value	*P* Corrected
1876	L precentral gyrus/knob (4), M1	−36	−23	49	Inf.	0.000
	L precentral gyrus (4/6), PMdc	−46	−15	52	Inf.	0.000
1881	R anterior cerebellum	20	−53	−19	Inf.	0.000
	Cerebellar vermis	4	−66	−7	Inf.	0.000
210	L parietal/temporal operculum (40/42), S2	−51	−26	14	Inf.	0.000
379	L anterior cerebellum	−28	−42	−25	7.79	0.000
265	Medial frontal gyrus (6), SMAc	−2	−4	46	6.82	0.000
15	L superior parietal lobule (5)	−24	−47	66	6.51	0.000
30	R posterior central gyrus (1, 2, 3)	53	−26	53	5.56	0.000

Cluster size = number of voxels; *x*, *y*, *z* = stereotaxic coordinates; *P* corrected = voxel level significance corrected for multiple comparisons; inf. = infinite.

Figure 5. Brain areas activating more during the movement tasks than the imagery tasks, according to Hanakawa et al. (2003).

TABLE 2. *Brain areas activated equally during the movement and imagery tasks*

Cluster Size	Locations (Brodmann area), Functional Areas	*x*	*y*	*z*	*Z*-Value	*P* Corrected
3593	L intraparietal sulcus (40/7)	−44	−42	57	Inf.	0.000
	L supramarginal gyrus (40)	−38	−43	37	Inf.	0.000
1401	L superior precentral sulcus (6), PMdr	−38	−1	55	Inf.	0.000
	L inferior precentral sulcus (6/44), PMv	−56	3	29	Inf.	0.000
2445	R intraparietal sulcus (40/7)	48	−40	54	Inf.	0.000
1959	R superior precentral sulcus (6), PMdr	37	1	57	Inf.	0.000
	Medial frontal cortex (6), SMAr	−2	8	49	Inf.	0.000
75	R posterior cerebellum	30	−65	−22	Inf.	0.000
53	L posterior cerebellum	−32	−67	−24	Inf.	0.000
40	L middle frontal gyrus (9/46), DLPFC	−42	38	26	Inf.	0.000
32	L inferior frontal gyrus (47)	−51	−18	−4	Inf.	0.000
35	R inferior frontal gyrus (47)	51	17	−4	6.92	0.000
26	L fusiform gyrus (18), visual association area	−28	−90	−6	6.75	0.000
7	L putamen	−24	−4	2	5.03	0.001

Cluster size = number of voxels; *x*, *y*, *z* = stereotaxic coordinates; *P* corrected = voxel level significance corrected for multiple comparisons; inf. = infinite.

Figure 6. Brain areas activating equally during the movement and imagery tasks, according to Hanakawa et al. (2003).

TABLE 3. *Brain areas activated more during the imagery tasks than the movement tasks*

Cluster Size	Locations (Brodmann area), Functional Areas	*x*	*y*	*z*	*Z*-Value	*P* Corrected
150	L dorsal parietal cortex/precuneus (7)	−24	−69	53	6.21	0.000
94	R posterior superior parietal cortex/precuneus (7)	22	−69	53	6.04	0.000
6	L precentral sulcus/middle frontal gyrus (6)	−47	4	48	5.10	0.006

Cluster size = number of voxels; *x*, *y*, *z* = stereotaxic coordinates (Montreal Neurological Institute template); *P* corrected = voxel level significance corrected for multiple comparisons; inf. = infinite.

Figure 7. Brain areas activating more during the imagery tasks than the movement tasks, according to Hanakawa et al. (2003).

These results (**Figures 5**, **6, 7**) go along with the findings of Solodkin et al. (2004) on the reporting of an overlap between areas activated during MP and during mental representation, i.e., MI. There is a functional equivalence between the mental process in which the subject pictures himself performing a given task and the actual motor performance (Lacourse, et al., 2005).

Previous studies such as Gao et al. (2011), Gerardin et al. (2000) have shown similar brain regions activated during motor execution and imagery, such as supplementary motor area (SMA) and premotor cortex (PMC). Also, common neural networks were reported, including bilateral PMC, parietal areas and also regions like the basal ganglia and cerebellum. Accounting for these studies, one can say that MP and MI share a common neural substrate.

The neural overlap between MI and MP is more clear in SMA and PMC (Geradin et al., 2000) with higher activity in the ventral part of the premotor cortex (PMv), the part responsible for movement planning, during MI (Guillot et al., 2014).

The increased activity of rostral supplementary motor area (SMAr) and rostral portion of the dorsal premotor (PMdr) has been reported in MI tasks (Gerardin et al., 2000) and both brain regions do not connect directly to primary motor cortex (M1) nor spinal cord, but are closely connected to the prefrontal cortex (PFC) (Hanakawa et al., 2003). The PFC, SMAr, and PMdr activation was recorded with a very similar temporal profile in both imagery and actual movement experiments allowing to conclude that there is a similar functional role of the PMd with the PFC in motor imagery and planning more than in the actual motor performance (Hanakawa et al., 2003).

Using an overlapping region as a neurofeedback target area would represent an opportunity to study the impact of neurofeedback (based on motor imagery) underlying both networks (Hui et al., 2014).

3.3.4. Motor cortex rt-fMRI-NF

3.3.4.1. rt-fMRI-NF activation - primary motor cortex

Berman et al. (2012) designed a real-time fMRI-based neurofeedback experiment in which the main objective was to test if subjects could learn to volitionally modulate brain activity within motor areas, since it would represent a therapeutical alternative for motor rehabilitation after a central nervous system injury.

Results show that subjects learned to modulate brain activity during the course of one session, within the ROI, the primary motor cortex (M1). There were two types of tasks: finger tapping and tapping imagery task. During a finger-tapping task in subjects quickly learned to self-modulate M1 activity. However, the participants were not able to successfully modulate M1 BOLD signal during motor imagery tasks. This last result adds to the existing controversial of the role of primary motor area in motor planning and imagery (Munzert, Lorey, and Zentgraf, 2009).

Finally, Berman et al. (2012) concluded that future rt-fMRI-NF investigations involving motor imagery may have better results if the main focus shifts to alternative motor cortex areas, such as PMC or even by exploring self-modulation of motor network connectivity.

3.3.4.2. rt-fMRI-NF activation - premotor cortex

Xie et al. (2015) focused his study on self-regulation of right premotor cortex (rPMC) activation and its effects on functional connectivity of motor related areas based on a MI paradigm. The results allowed to conclude, using graph theory, that there were alterations in the functional connectivity between PMC and regions within motor network. Feasibility of self-modulation in PMC areas using mental imagery of movement, i.e., MI, as well as the notion that motor imagery training might help participants to improve behavior performance by neurofeedback of targeted areas, were both confirmed.

3.4. Transition to motor cortex connectivity based fMRI-NF

Zilverstand et al. (2014) aimed at investigating the potential of providing functional correlation (computed from short-window time course data) as feedback in a neurofeedback experiment. The paradigm used was a simple motor task. Additionally, the authors investigated the potential of using a hypothesis-driven, computationally inexpensive method, the windowed seed-based correlation.

The ability to detect subtle changes in task performance with block-wise functional connectivity measures was evaluated with a finger tapping task that was systematically modulated in terms of tapping speed and demand on bimanual coordination, thus combining two aspects of task difficulty. The authors observed that windowed correlation provides valid information on certain task aspects, in agreement with was previously described in the literature of motor cortex.

The increasing demand on bimanual coordination or tapping speed during finger tapping leads to higher functional connectivity. There is also a consistency with previous results that reported an enhanced interhemispheric coupling during early stages of motor skill learning, when task difficulty is higher. The authors concluded that fMRI-based functional connectivity measures may provide a better indicator for an increase in overall motor task difficulty than activation level-based measures.

Materials and Methods

4.1. Participants

10 Healthy subjects performed the FC-based rt-fMRI NF experiment proposed. The age of the volunteers was comprised between 23 and 33, seven were male and three female, and had different levels of familiarity with fMRI and neurofeedback experiments (some never performed any rt-fMRI-NF experiments while others had previous experience).

All experiments were preceded by a 30 minute pre-scan training session in which each subject got acquainted with the fMRI protocol, the reference tasks and was answered any questions. After the fMRI session, all subjects answered a 6 questions debriefing questionnaire, in which the participants identified how they felt and what were the strategies used during the experiment (**Annex II**).

Their motor imagery Ability was assessed using the Movement Imagery Questionnaire-3 (MIQ-3) from the work of Mendes et al. (2016) (**Annex I**).

Two additional subjects performed pilot studies to optimize the protocol. The specificities of the pilot studies are described in **Section 4.3**.

4.2. Experimental Protocol

Each session consisted of an anatomical run and six functional runs - a functional localizer, and five imagery runs. The first imagery run is also known training run (or baseline). This run is followed by three neurofeedback runs. Finally, the last functional run is usually known as transfer run.

4.2.1. Structural run

Each scanning session includes the acquisition of a high-resolution magnetization-prepared rapid acquisition gradient echo (MPRAGE) sequence for co-registration of functional data (176 slices; Echo Time (TE): 3.42 ms; Repetition time (TR): 2530 ms; voxel size 1.0×1.0×1.0 mm^3; Flip Angle (FA): 7°; Field of view (FOV): 256×256).

4.2.2. Functional runs

Functional images focused motor-related areas (frontal, parietal areas). The acquisition parameters were 26 slices, in-plane resolution: 3×3 mm2, FOV: 210×210 mm, slice thickness: 3.5 mm, FA: 75°, TR = 1500 ms and TE = 30 ms.

The stimuli were presented with a 800 x 600 pixels resolution, on a 70 x 39,5 cm LCD monitor, with a resolution of 1920 × 1080 pixels (refresh rate of 60Hz), and projected to the participant through a mirror. The distance between the eyes and the mirror is approximately 13 cm. The LCD is placed 156 cm from the participant resulting on a vertical visual angle of approximately 8º.

4.2.2.1. Functional localizer

To *functionally* localize our neurofeedback target regions, we used a mapping procedure combining imagining movement as well as actual performance.The idea was to define PMC **bilaterally** following the task proposed in Xie et al. (2015). The procedure includes two activation conditions, motor imagery (MI) and motor performance (MP) and baseline periods in a randomized block design. Further information concerning PMC is on **Section 3.3.1**.

The mapping procedure proposed includes a total of 17 blocks - nine baseline blocks, four MI blocks and four MP blocks; each block lasts 30 seconds (i.e. 20 points considering TR of 1.5s). The total duration of the localizer is 8 minutes and 30 seconds (17 blocks * 30 seconds = 510 seconds/1.5 = 340 points).

At the beginning of each block, the instruction is presented to the participants on the screen during 3 seconds. During the MP blocks, the participant is instructed to execute a finger tapping sequence - 1-2-1-4-3-4 (the numbers represent the fingers: 1 being the middle finger and 2 the index finger of the left hand and 3 the index and 4 the middle finger of the right hand) - at a specific frequency (e.g. 2 Hz) and during the MI blocks, the participant is asked to imagine the same sequence.

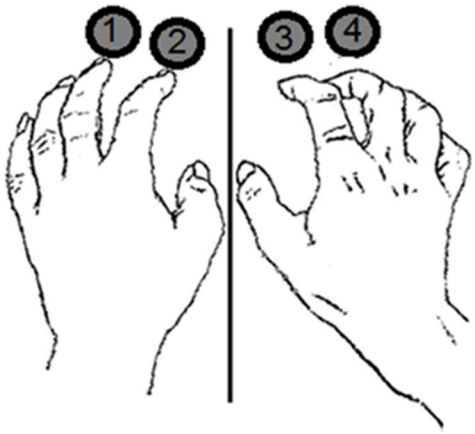

Figure 8. Schematic representation of finger position for the finger tapping task performed during Localizer run.

The bilateral ROIs (rPMC and lPMC) are selected according to the contrast MI greater than the Baseline considering the online General Linear Model (GLM) produced by Turbo BrainVoyager (TBV) 3.2 software (Brain Innovation, Maastricht, The Netherlands). The voxels were selected based on a statistical threshold and anatomical principles - anterior to the central sulcus and superior to the Sylvian fissure, caudal parts of the superior frontal gyrus and middle frontal gyrus and in the rostral part of the precentral gyrus not occupied by the primary motor cortex (M1).

4.2.2.2. Imagery runs

During the imagery runs, the participant was instructed to perform a motor imagery task. The protocol includes two different conditions: **i.*Increase*** *connectivity blocks where the reference task is the bimanual motor imagery movement*, **ii.*Decrease*** *connectivity blocks in which the subjects were asked to decrease the feedback value by not activating premotor cortex areas*.

Every imagery run is composed by 17 blocks (8 **i.*Increase*** blocks alternating with 9 **ii.*Decrease*** blocks), each block with the duration of 30 seconds, totaling 510 seconds (340 TR).

In condition **i.Increase** blocks, visual instruction was presented in the LCD monitor, composed by a simple command that asked the participant to increase the correlation between bilateral PMC. There is also a auditory cue – beep – at the 15 second mark, signaling the middle of the condition block At the beginning of the blocks from condition **ii.Decrease**, a visual command appeared, asking

the participant to decrease their bilateral PMC connectivity, i.e., decrease the feedback value. In both conditions, condition name maintains visible during the length of the block.

This protocol is a result of an optimization period consisting of four pilot studies (a comprehensive descriptions of this process is presented in **Section 4.3**).

Training run

After the definition of the neurofeedback target, the participant performed a training run without feedback. The block design is similar to the Neurofeedback runs, allowing to have a reference value.

Neurofeedback runs

The participants performed three rt-fMRI-NF runs, in which they were instructed to modulate their interhemispheric connectivity in a block design paradigm. During the run, the feedback was presented indicating the connectivity level.

The participants were given the freedom to explore different approaches since neurofeedback is an individually tailored framework and depends on the personal experience (Sitaram et al., 2017). However, this exploration is always based with the reference tasks given beforehand and explained in **Section 4.2.2.2** that result from the literature review of motor cortex (**Section 3.3.2** and **3.3.3**).

Transfer run

Finally, after the three neurofeedback (NF) runs, the participants performed a control run. The block design is similar to the NF runs. The participant was instructed to perform a similar motor imagery task as in the previous NF runs but without the feedback information.

The transfer run is performed to verify the contribution of feedback in the volitional control of the interhemispheric connectivity, and analyze the differences between situations with and without the feedback provision.

4.3. Protocol Optimization to achieve modulation of functional connectivity

During the optimization of the experiment, different challenges were met and several adjustments were necessary. Different parameters were adjusted, such as the proposed mental imagery task/strategy, number and structure of experimental conditions, etc.

To this end, we performed four different pilots (27th of June, 2016, 12th of September, 2016 and two on the 4th November, 2016).

In all pilot studies three different conditions were considered in the imagery runs: **Bimanual condition** blocks where the reference task is the bimanual motor imagery movement, **Unimanual condition** where the reference task is the unimanual imaginary movement and **Baseline** in which the subjects were asked to remain in a resting state (please note that the final version of the protocol does not present condition **ii.**).

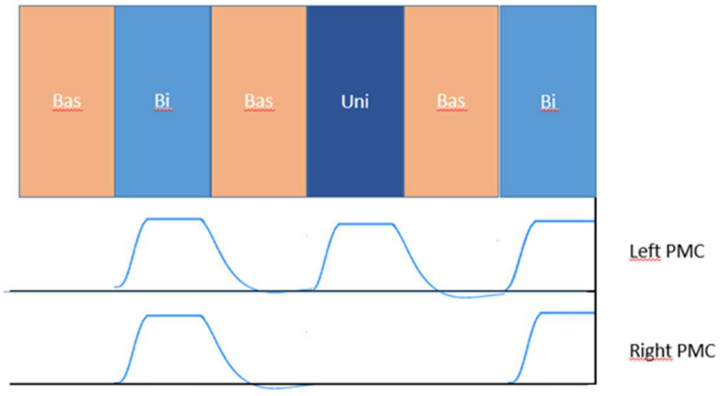

Figure 9. Schematics of the block design of the imagery runs with baseline ('Bas') blocks conditions with bimanual motor imagery ('Bi') and unimanual motor imagery ('Uni') as reference tasks. We considering the subject is imagining moving the right hand/finger in 'Uni' conditions. Below there is the expected curves of activation in the left and right PMC.

The **first pilot** main goal was to prove the feasibility of motor imagery paradigm as a suitable rt-fMRI-NF experiment.

The **second pilot** main goal was to test the best strategy to differentiate correlation distributions between conditions. We hypothesized that variations in the PMC BOLD signal within a condition block would maximize differences between conditions.

In that sense, in the neurofeedback runs, two strategies were tested. The first one was tested in the first two neurofeedback runs. The strategy consisted of the participant, within each **Bimanual** and **Unimanual** condition block, was asked to *imagine movement while gradually increasing and then decreasing the frequency of the imagined movements*. This assumption is made since according to Rao et al. (1996), the activation level within the whole motor network increases with increasing finger tapping speed.

In the third and last neurofeedback run, the participant was asked to gradually make the transition between *imagining more specific / fine movements and then imagine gradually coarser / wider movements* within each **Bimanual** and **Unimanual** condition block. Both strategies were facilitated with an inclusion of an auditory cue in the middle of every **Bimanual** and **Unimanual** condition.

Take note that, within the 30 second block, there is only two transitions: an increase in frequency/specificity followed by a decrease in frequency/specificity of imagined movements.

The **third and fourth pilots** were performed to validate the strategy with better results as to differentiate correlation distributions between conditions, as seen in the results **Chapter 5.1.2**. In these two pilots, the participants were asked to use the strategy of varying the frequency of imaging movement in all imagery runs.

Finally, to reach the optimized protocol used, the condition **Unimanual** with unimanual imagined movement as reference task, was discarded.

These changes in protocol were based in the results presented in **Sections 5.1.1**, **5.1.2** and **5.1.3**.

4.4. Online fMRI processing and feedback presentation

The online processing of the data required to compute and present the feedback in real time was performed using Turbo-BrainVoyager (TBV).

The software implements online 3D motion correction and alignment between functional runs. As volumes continue to arrive, they are incrementally analyzed using an online GLM based on a recursive squares algorithm [2].

4.4.1. ROI selection

The first step is the identification of the two ROIs (lPMC and rPMC) based on the Localizer run. Through the activation maps created by the GLM, (see **Figure 10**), is possible to see which brain areas activate more in MI than in Baseline. Both lPMC and rPMC are one of those areas and with anatomical references explained previously in **Section 3.3** is possible to select bilateral PMC as the neurofeedback targets.

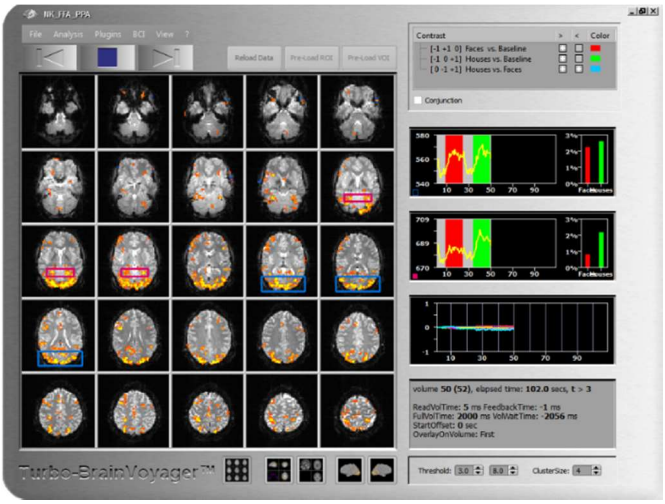

Figure 10. Overview of TBV framework. The statistical activation maps calculated by the online GLM in the different slices of the brain on the left, the different contrasts possible in the top-right, the BOLD response for each of the two ROIs selected in the middle-right and the 3D motion correct parameters in the bottom-right [3].

4.4.2. Feedback calculation

With both ROIs selected, TBV allows for the extraction of the mean BOLD value of those ROIs, identified in the Localizer run. Based on the ROIs, TBV defines masks to extract data in the NF runs.

These values are used to calculate the functional connectivity feedback. It is calculated using an 8 point sliding window Pearson's Correlation Coefficient, **Equation 1,** between ROIs BOLD signal. We believe that a size of 8 points represents compromise between the block size and necessary information. The feedback was updated in every single point.

$$r = \frac{\sum_{i=1}^{n}(xi - \bar{x})(yi - \bar{y})}{\sqrt{\sum_{i=1}^{n}(xi - \bar{x})^2} \cdot \sqrt{\sum_{i=1}^{n}(yi - \bar{y})^2}}$$

$$= \frac{cov(X, Y)}{\sqrt{var(X).var(Y)}}$$

Equation 1. Calculation of Pearson's Correlation Coefficient being x and y the mean BOLD signal of both ROIs and n=8.

The values of correlation range between -1 to 1 and are presented to the subject in the form of a thermometer.

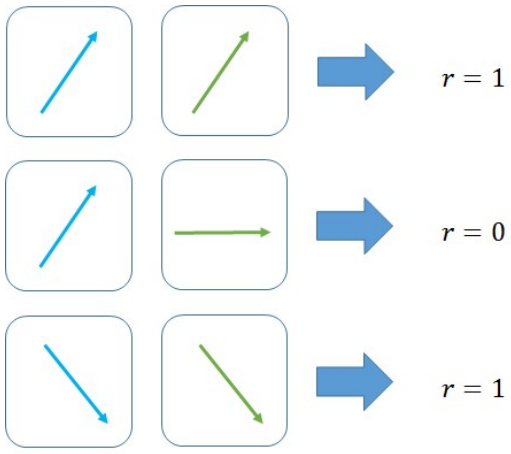

Figure 11. Schematization of Pearson Correlation Coefficient values accordingly to the behavior of the data points in two variables, differentiated by blue and green colors.

To extract the noise normal to fMRI data and windowed correlation using Pearson Correlation (Zhang, Tian, and Zhen 2007) and to avoid presenting feedback with rapid variations that could lead to frustration and fatigue amongst the participants, a three point a smoothing function is used before computing every voxel correlation coefficient.

Explained in the **Figure 11**, if the two ROIs mean BOLD signal values, in the eight point interval, have the same slope, r will have a positive value +1. This is valid for both increases and decreases in mean BOLD value. If one of the ROI does not activate, its BOLD signal tends to remains constant and therefore the coefficient value will approach zero. If f the behavior is symmetric, the coefficient will tend to have a negative value -1.

The subjects are then asked to fill the thermometer in up-regulation blocks, with correlation values approaching one and to empty it, in down-regulation blocks with correlation values tend to zero, **Figure 12**.

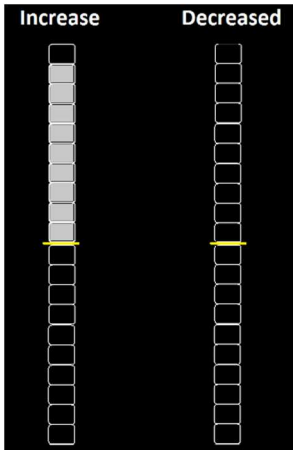

Figure 12. Neurofeedback and instructions presented to each participant in both **i.Increase** and **ii.Decrease** conditions.

4.5. Offline fMRI processing

Offline fMRI analyses are used to determine the correct position of the ROIs and to extract the temporal response through the runs. Based on these extracted data, comparisons between the correlation coefficient distributions between conditions are possible to conclude on whether each experiment was successful.

The analysis used was Brain Innovation's BrainVoyager (BV), a highly optimized software package for the analysis and visualization of functional and structural magnetic resonance imaging.

4.5.1. Preprocessing

The preprocessing stages takes the raw functional MRI data and applies various images and signal processing techniques, reducing noise and artefacts. It is recognized that these steps are not independent and that some power is lost in the statistical analysis by ignoring the interactions between these preprocessing steps. This sequence is crucial on improving the power of subsequent analysis and therefore validating the statistical inferences. (Faro and Mohamed 2010).

Slice Scan Time Correction

A functional volume is not covered all at once, but rather with a sequence of two dimensional (2D) slices. A last slice of one functional volume will be measured 1.5 seconds after the first one. Slice Scan Time Correction shifts the data of each slice in time to the same time point as when the first slice was scanned. This makes if the whole volume would have been measured at the same moment in time as the first slice [4].

Motion Detection and Correction

During any run, any type of head movements strongly decreases the quality of the fMRI data. Considering the chosen voxel size, any movement of the subject on the order of millimeters will cause voxels to measure other neighboring brain areas.

Motion Detection and Correction is done by selecting one functional volume from a reference run in the same scanning to which all other functional volumes are aligned. This algorithm analyzes how a source volume should be translated and rotated in order to better align with the

reference volume. It considers head movements as a rigid body describing it by 6 parameters, three translational and three rotation, estimated iteratively, **Figure 13** [5].

Although head motion can be corrected in image space, displacements of the head reduce the homogeneity of the magnetic field, which is fine-tuned ("shimmed") prior to functional scans for a given head position [5].

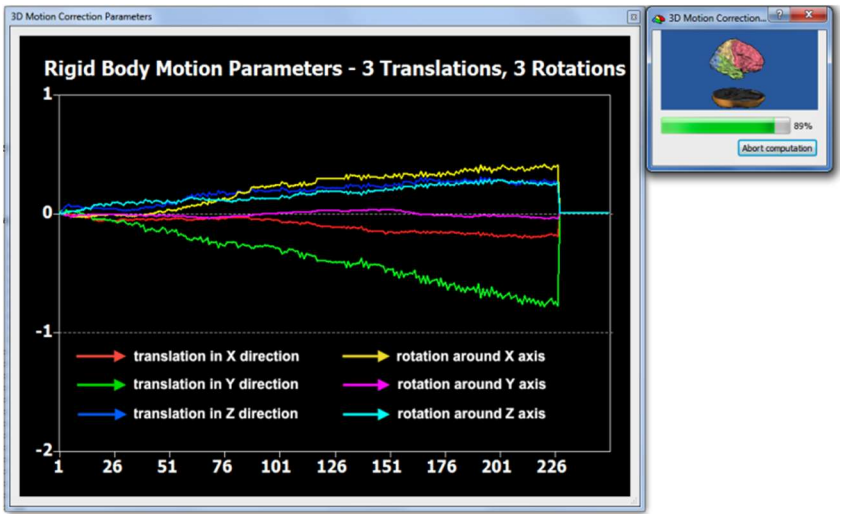

Figure 13. 3D motion correction performed in a functional run, with the variation along the 6 parameters throughout the length of the run [5].

Temporal High-Pass Filtering

Physiological noise, including cardiorespiratory effects and head movement, as well as scanner-related noise will cause voxel time courses in fMRI data to show low-frequency drifts that can reduce greatly the data analysis statistical power [6].

The removal of these drifts is done by using a high-pass filter, letting high frequency data (that includes activity related to the stimulus) go through and removing low frequency data in where the drifts are included [6].

Anatomical-Functional Coregistration

As it is described in **Section 4.2**, there are two types of runs: the structural and the functional. The structural provides anatomical information about the structures of the brain with higher spatial resolution. The functional provides the response profile across experimental conditions of the brain regions inside its FOV, **Figure 14**.

Anatomical-Functional coregistration allows to align functional and anatomical data sets and therefore relate brain activity to anatomical locations, with a highly precision [7].

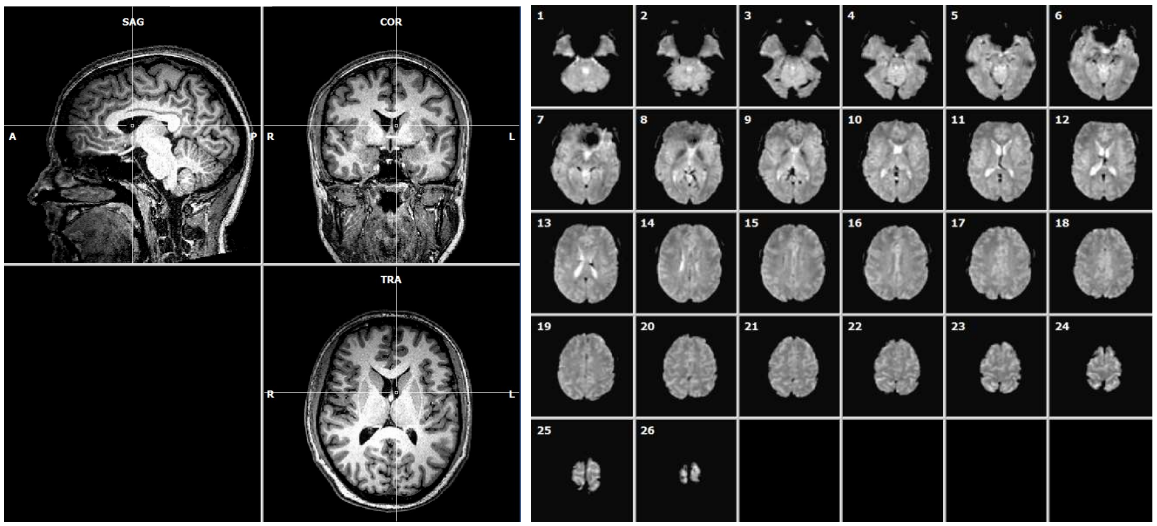

Figure 14. Example of an anatomical file, on the left and a functional file containing the information from the 26 slices selected, on the right. Both files are co-registered in BV.

Brain Normalization - ACPC and Talairach

With the main goal of relating a combination of coordinates to a specific brain area it was essential to use a normalized spatial referential, the Talairach Space (TAL), originally defined by Talairach and Tournoux (1988).

For each participant, in order to transform the brain from its native space to TAL, the anterior commissure (AC) was first located, serving as the point of origin in where all coordinates value as zero.

The anatomical image of the brain suffered a consequential rotation around a plane formed by AC and the posterior commissure (PC), the AC-PC plane that was used as one of the axis in TAL space.

To fully transform to TAL space, 12 sub-cuboids were formed after a cuboid defined in the AC-PC space using another reference points as the borders of the cerebrum expanded or shrunken in order to correspond to the sub-cuboid of the standard Talairach brain [8]. In TAL space, all three coordinates (x, y, and z) are specified in millimetres.

Creation of Volume Time Course Data

Linking the functional information to the anatomical image in TAL space, a volume time course of each functional run present in the protocol into TAL space is created. This opens up the possibility of verifying the BOLD signal response across the entire run of normalized anatomical regions [9].

4.5.2. General Linear Model

To confirm the regions selected online, we need to identify the regions that have a higher activation for the MI condition compared to Baseline condition. To this end, we used a statistical framework known as GLM.

Most of the statistical parametric maps used to test hypotheses about regionally specific effects in neuroimaging data are based on linear models, for example ANCOVA, correlation coefficients and t test. Since these examples are all special cases of the general linear model, Friston et al. (1994) considered the possibility of implement them, amongst other, within a unified framework.

GLM is mathematically identical to a multiple regression analysis but suitable for both multiple qualitative and multiple quantitative variables. Because of this flexibility, GLM has become the most used tool for fMRI data analysis after its introduction into the neuroimaging community by Friston and colleagues (Friston et al., 1994).

In BrainVoyager, GLM refers to its univariate version, since there is a univariate dependent variable, the time course of each voxel, in which a separate statistical analysis is performed. GLM aims

to explain the variation of the voxel time series using a linear combination of predictor functions that correspond to the predicted/expected BOLD response for each condition in the experimental protocol, **Figure 15**. This optimal fMRI response is the convoluted step signal - defined by ones at time points that correspond to the specific condition to be "on" and zeros in all other time points - with the hemodynamic response function [2].

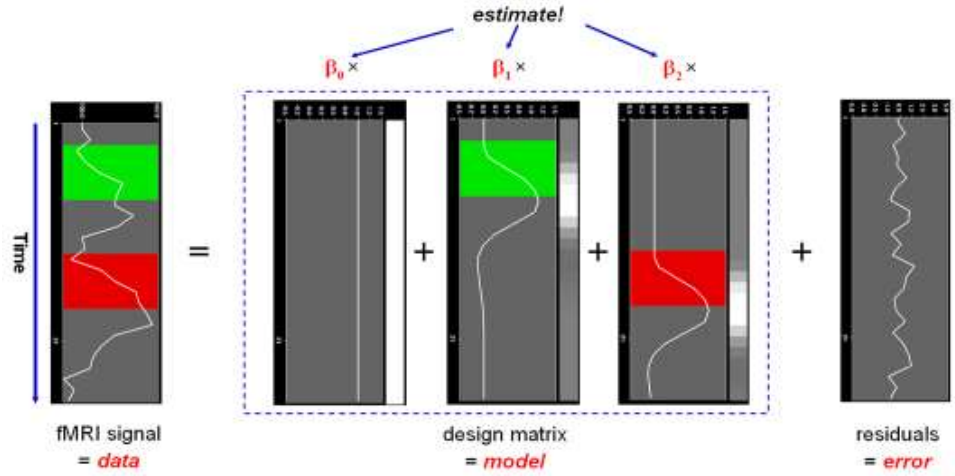

Figure 15. The GLM approach at statistically explain the BOLD response in each voxel with three predictor functions that form the model, already convoluted with the HRF and the noise/residuals that comes from the deviation between fMRI signal and the linear combination of the ideal response.

This approach can be described using the matrix notation and the concept of design matrix and the predictor beta values that are used in GLM diagnosis.

$$\begin{bmatrix} y_1 \\ \vdots \\ \vdots \\ \vdots \\ y_n \end{bmatrix} = \begin{bmatrix} 1 & X_{11} & \cdots & \cdots & \cdots & X_{1p} \\ \vdots & \vdots & \vdots & \vdots & \vdots & \vdots \\ \vdots & \vdots & \vdots & \vdots & \vdots & \vdots \\ \vdots & \vdots & \vdots & \vdots & \vdots & \vdots \\ 1 & X_{n1} & \cdots & \cdots & \cdots & X_{np} \end{bmatrix} \begin{bmatrix} b_0 \\ \vdots \\ \vdots \\ \vdots \\ b_p \end{bmatrix} + \begin{bmatrix} e_1 \\ \vdots \\ \vdots \\ \vdots \\ e_n \end{bmatrix}$$

Equation 2. Representation of GLM with the voxel time course as the y variable, the set of predictors in the form of matrix, the design matrix, linearly combined with the beta values, also called the predictors and the residuals as vectors.

Single Study Analysis

For a single subject, in order to verify if a voxel activation in motor imagery (MI) is significantly different from its activation in Baseline, we considered a null hypothesis that stated that the beta values of the two conditions would be the same, meaning H0: b1 = b2 or equivalently H0: (+1)b1 + (-1)b2 = 0 [10].

These [+1 -1] values that multiply the beta values for each condition are denominated as a contrast vector c. With the following t statistic, the contrast vector can be tested:

$$t = \frac{\mathbf{c}'\mathbf{b}}{\sqrt{Var(\mathbf{e})\,\mathbf{c}'(\mathbf{X}'\mathbf{X})^{-1}\mathbf{c}}}$$

Equation 3. Statistic t-test where the numerator is the scalar product of the beta and contrast vectors and the denominator is the standard error of this product, the variability of the estimate due to noise fluctuations [10].

For confirming the selected ROI, considering the conditions [‘Motor Performance”, “Motor Imagery”, “Baseline”’] we use as contrast vector [0 1 -1].

For the one sided Ha (alternative hypothesis): MI> Baseline, if the obtained p value is smaller than 0.05 and if the t value is positive, the null hypothesis is rejected [10] and statistical maps appear such as in **Figure 16** containing brain areas more activated during MI than Baseline.

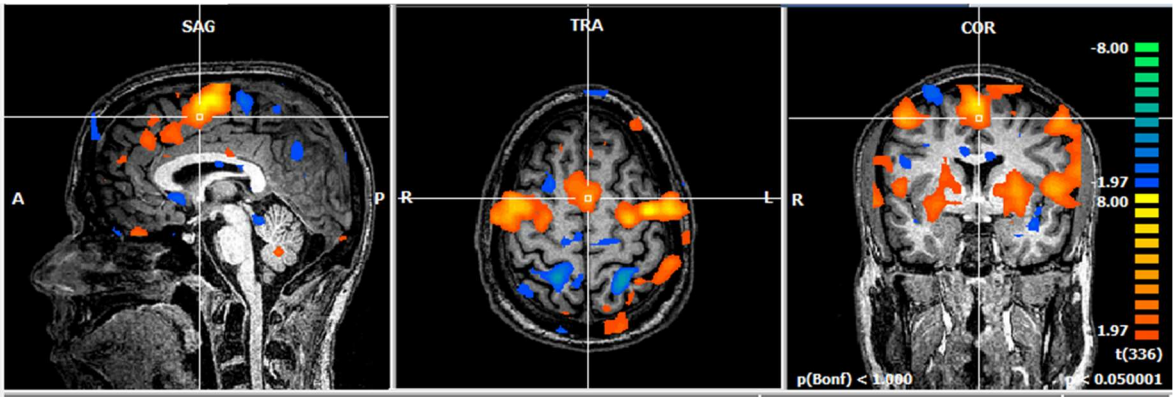

Figure 16. Statistical activation map of the overlaid GLM, between two conditions (MI greater than Baseline), with p<0.05.

Group Analysis - Random Effects

In the Random Effects (RFX) group analysis, individual subjects in a multi-subject studies are considered to be representative sample of a population of the study. If group effects are statistically significant at random effects level, the findings from the sample of subjects could be generalized to the population of the study.

Usually, RFX group analysis is divided in two steps, in which the first treats each subject independently and calculates statistical tests according to the research question in the study and the second oversees the distribution of the statistical significance of each individual, and returns a value that allows to conclude if the results can be generalized to the population. The error variance, in RFX group analysis, is estimated by the variability of subject specific effects across the population [11].

4.6. Statistical analysis

The main goal of this statistical framework is to compare the correlation distributions between conditions **i.Increase** and **ii.Decrease** after the extraction of the mean BOLD time series for each ROI, it is possible to compute the correlation. Correlation was computed using **Equation 1**, explained in **Section 4.3.2**.

To this end, instead of using all the points from each condition (i.e. 20 points from each block), we preferred to only use the final 12 correlation values from each block. The rationale is that the first 8 points represent a mixture of data between both conditions (points from the previous block – different condition – would be considered).

Then, we compare the correlation distribution between conditions using only BOLD signal from time points in which the subjects has access to feedback with mostly information regarding the current condition block.

For this effect, it is necessary to determine which statistical analysis is going to be performed. Firstly, it is necessary to prove if the correlation values follow a normal distribution or not. It was used

the **Lilliefors test**, since the null hypothesis does not specify the expected mean and variance of the distribution (Lilliefors, 1967).

Assuming the independency of each run, within a rt-fMRI-NF session and according to the results, if correlation values follow a normal distribution, an **independent t-test** will be performed, to determine the probability of a significant difference between the **i.Increase** and **ii.Decrease** correlation measures. However, if normality test fail, **Wilcoxon Mann-Whitney test** will be performed. This non-parametric statistical test, evaluates the null hypothesis that correlation distributions of both conditions are samples from the same distribution and has the **median** as measure of central tendency that allow to verify which condition has a higher sample of correlations.

Results

5.1. Pilot studies and protocol optimization

We first present the results of the four pilots performed that led to the final protocol.

5.1.1. First Pilot

This first pilot was a feasibility test of an rt-fMRI-NF motor paradigm, explained in **Section 4.3**.

Localizer run

First we confirmed the position of the ROIs offline. **Figure 17** highlights the correspondence between the ROIs selected online and the GLM (as described in **Section 4.4.2**). There is a larger number of active voxels corresponding to the lPMC, which corresponds to the subject's dominant motor hemisphere (the participant was right-handed).

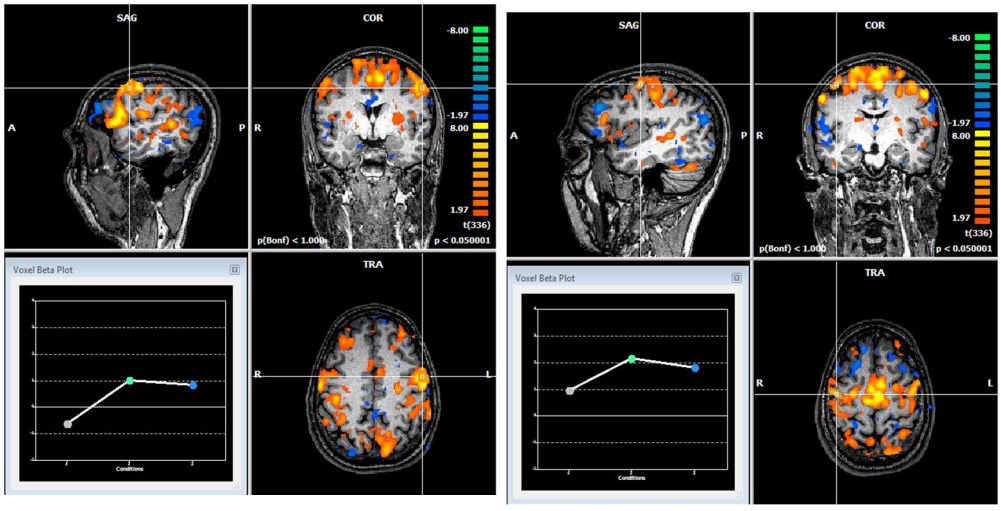

Figure 17. First Pilot Localizer run activation map with p<0.05 and contrast MI greater than Baseline with the overlap of the ROIs selected online through TBV (on the left the lPMC and on the right the rPMC). Also present the plot of their Beta regression coefficients activation in the three conditions - Baseline (gray), Motor Imagery (green) and Motor Performance (blue).

The number of voxels of the ROIs obtained online and their anatomical location in TAL are presented in **Table 1**.

Table 1. *Voxel size and position of the ROIs selected online in the Localizer run.*

Region of Interest	Voxels	Talairach coordinates(x,y,z)
lPMC	1140	(-51, -3, 41)
rPMC	425	(40, -12, 53)

Imagery runs

As described in **Section 4.5**, in order to determine if the correlation distribution from the different conditions in all imagery runs are different we performed a normality test. The result of this test (present in **Annex III)** show that most runs do not follow a normal distribution.

As a reminder, as explained in **Section 4.3** conditions are **Bimanual** blocks where the reference task is the bimanual motor imagery movement, **Unimanual** blocks where the reference task is the unimanual imaginary movement and **Baseline.**

Neurofeedback runs

The results of the **Wilcoxon test** performed to determine if correlation distributions are significantly different in each NF run are in the **Table 2**. To best understand which of the three conditions (described in **Section 4.3.**) presents highest correlation values, the median values of each condition for each NF run are listed in **Table 3.**

Table 2. Wilcoxon Mann-Whitney test comparing correlation distributions from the three conditions present, in the three NF runs, with statistical significance of 0.05.

	Bimanual-Baseline			**Unimanual-Baseline**			**Bimanual-Unimanual**		
Run \ Condition	**p**	**h**	**stats**	**p**	**h**	**stats**	**p**	**h**	**stats**
NF run 1	5,12E-03	1	2,80E+00	8,59E-01	0	-1,78E-01	5,45E-02	0	1,92E+00
NF run 2	7,80E-01	0	-2,80E-01	9,76E-01	0	-2,95E-02	8,90E-01	0	-1,38E-01
NF run 3	1,47E-06	1	4,81E+00	4,58E-02	1	2,00E+00	1,13E-02	1	2,53E+00

Table 3. Median values for the correlation distribution for the three conditions - **Bimanual, Unimanual and Baseline** - in the three NF runs.

	Median		
Run \ Condition	**Bimanual**	**Unimanual**	**Baseline**
NF run 1	0,66	0,41	0,44
NF run 2	0,48	0,48	0,53
NF run 3	0,64	0,42	0,35

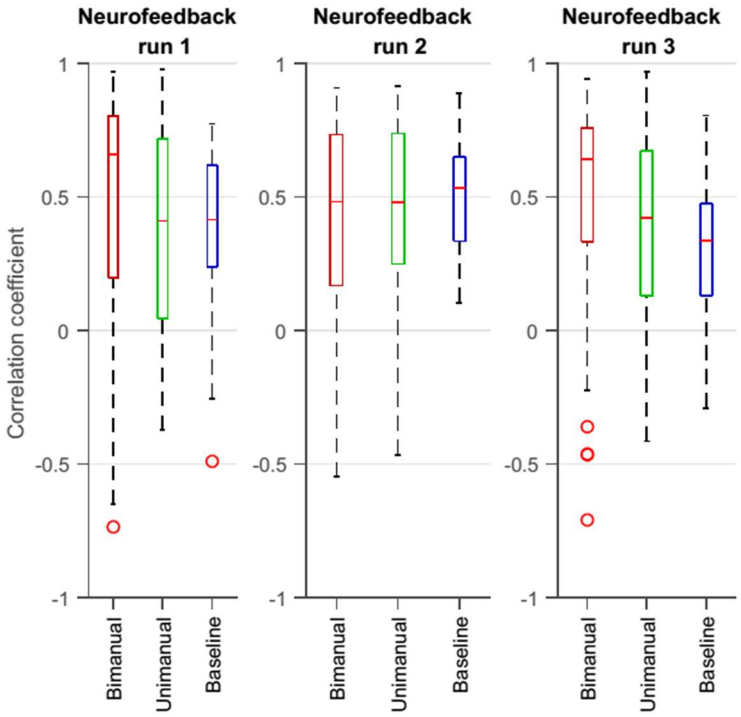

Figure 18. Correlation distribution conditions in the NF runs of the first pilot.

In the **Table 2**, results show a greater difference between **Bimanual** and **Baseline** conditions, statistically significant in two out of three NF runs. In this runs, condition **Bimanual** consistently showed the highest correlation values. During all three NF runs conditions, **Unimanual** and **Baseline** alternately showed the lowest values, as visible in **Figure 18**.

To better understand the values of correlation and the difference of distribution between them, we inspected how BOLD signal variated throughout the activation conditions **Bimanual** and

Unimanual. **Figure 19** represents the Event Related Averaging (ERA), the mean values of BOLD for each time point, for the three NF runs.

.

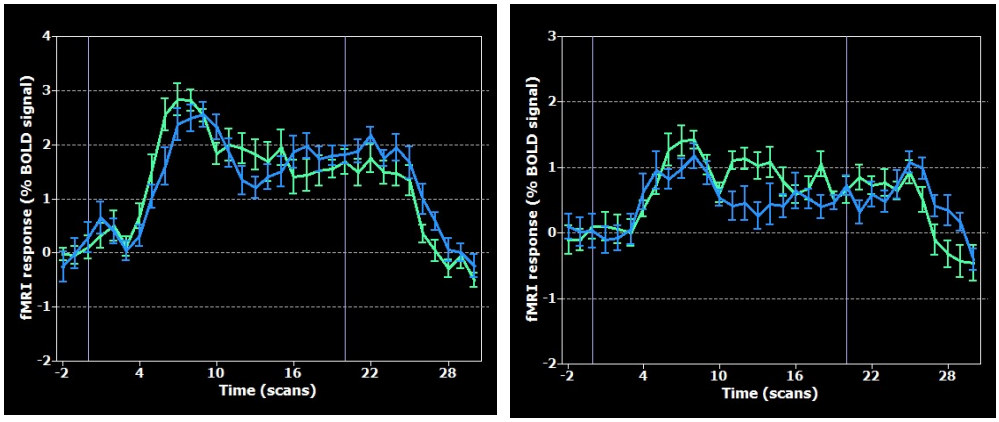

Figure 19. ERA of the three NF runs in the lPMC (on the left) and in the rPMC (on the right). The green curve represents ERA of condition **Bimanual** and blue represents ERA of condition **Unimanual.**

In **Figure 19** it is visible, for lPMC and rPMC, an initial increase in BOLD signal in the beginning of the block and a consequent *"plateau"* in activation until the end of the 20 point mark. Both ROIs BOLD signal decreases after the end of the activation condition, already during the **Baseline** condition.

Training and Transfer runs

The results of the **Wilcoxon test** performed to determine if correlation distributions are significantly different in both Training and Transfer run are in the **Table 4** with the medians presented in **Table 5.**

Table 4. Wilcoxon Mann-Whitney test comparing correlation distributions from the three conditions present, in both Training and Transfer runs, with statistical significance of 0.05.

	Bimanual-Baseline			**Unimanual-Baseline**			**Bimanual-Unimanual**		
Run \ Condition	**p**	**h**	**stats**	**p**	**h**	**stats**	**p**	**h**	**stats**
Training	6,84E-03	1	2,70E+00	8,94E-02	0	1,70E+00	6,76E-01	0	4,18E-01
Transfer	4,14E-03	1	2,87E+00	9,18E-01	0	-1,03E-01	1,36E-03	1	3,20E+00

Table 5. Median values for the correlation distribution for **Bimanual, Unimanual and Baseline** conditions in both Training and Transfer runs for the First Pilot.

	Median		
Run \ Condition	**Bimanual**	**Unimanual**	**Baseline**
Training	0,52	0,48	0,48
Transfer	0,57	0,27	0,34

The separation from the conditions **Bimanual** and **Baseline** was present in both runs and the **Bimanual** and **Unimanual** conditions in the Transfer run. Correlation values were highest for **Bimanual** and lower for **Unimanual**.

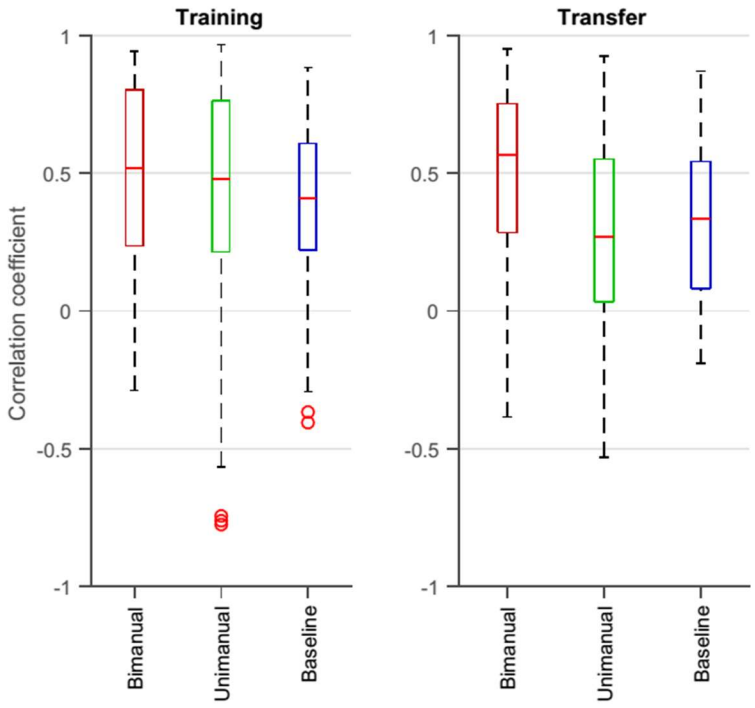

Figure 20. Correlation distribution between conditions in the Training and Transfer runs of the first pilot.

Figures 21 and **22** show the ERA for both ROIs BOLD signal, for a better understanding of the correlation values.

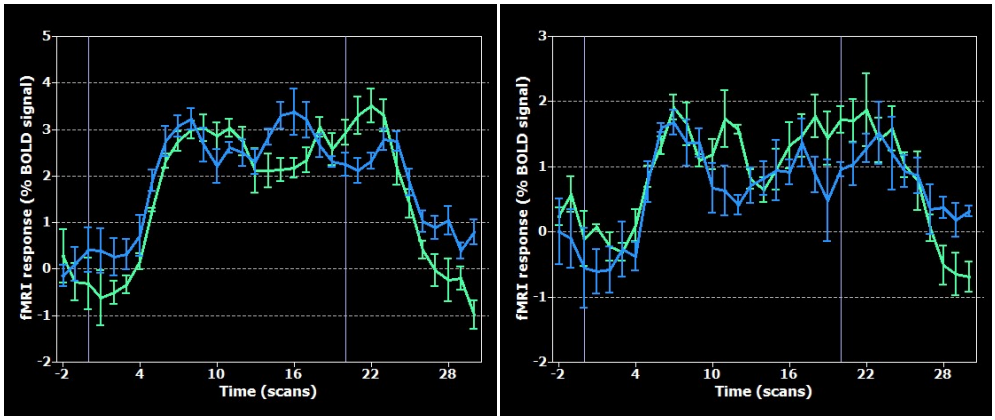

Figure 21. ERA of the Training condition BOLD response for the lPMC (on the left) and for the rPMC (on the right). The green curve represents ERA of condition **Bimanual** and blue represents ERA of condition **Unimanual.**

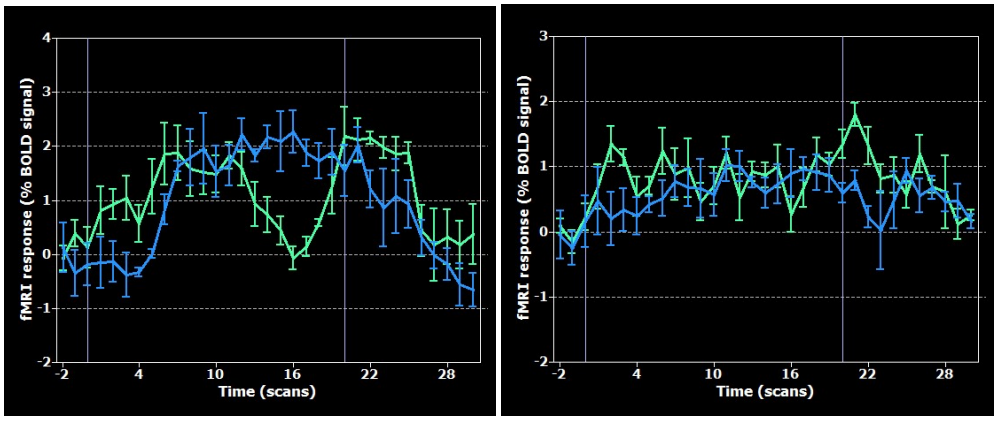

Figure 22. ERA of the Transfer condition BOLD response for the PMC (on the left) and for the rPMC (on the right). The green curve represents ERA of condition **Bimanual** and blue represents ERA of condition **Unimanual.**

In the Training and Transfer runs, ROIs BOLD response was similar to the NF runs, only with a decrease around the middle of the block in activity in the **Bimanual** condition in the Transfer run as well as a lower activation in the rPMC for both conditions.

Shortcomings

The correlation pattern was not as expected. In condition **Bimanual**, bilateral PMC activation is constant after the initial peak correlation making correlation values decrease close to zero. As consequence, low values of feedback are given, even though the subject is performing a motor imagery task.

Condition **Unimanual** presents an activation in both PMC. As consequence, correlation values differ from the low values we expected.

The decrease of BOLD signal in lPMC and rPMC happens after the end of the activation block. As a result, there is an increase in the correlation values and therefore high neurofeedback values presented to the subject, in condition **Baseline** even though there is no desire or intent to.

5.1.2. Second Pilot

The second pilot was planned to face the shortcomings of the first effort. The main goal of this second pilot was to find a strategy for optimizing the differentiation of all three conditions.

Please note **Figure 11**, with the properties of a sliding window Pearson Correlation Coefficient: if both mean ROIs BOLD signal increase or decrease, correlation values are high.

In order to maintain correlation values high, the expected BOLD response should consist of an initial signal increase, followed by a gradual decrease in the **Bimanual** condition. We also aimed to understand what happened to the **Unimanual** condition and its correlation distribution with this BOLD response. This **triangular shape** allows maximization of correlation in conditions with both PMC activation and allows for the BOLD signal to be low in the beginning of the next condition (**Baseline**).

The strategies used were to variate the frequency of imagined movement and variate the specificity of the imagined movement with use of an auditory cue in the middle of the block (**Section 4.3**).

Localizer run

We firstly confirmed the position of the ROIs offline. In the **Figure 23** we present a correct correspondence between the ROIs selected online and an activated voxel in the GLM. There is a larger number of active voxels corresponding to the lPMC, which corresponds to the subject's dominant motor hemisphere (the participant was right-handed), also visible in **Table 6**.

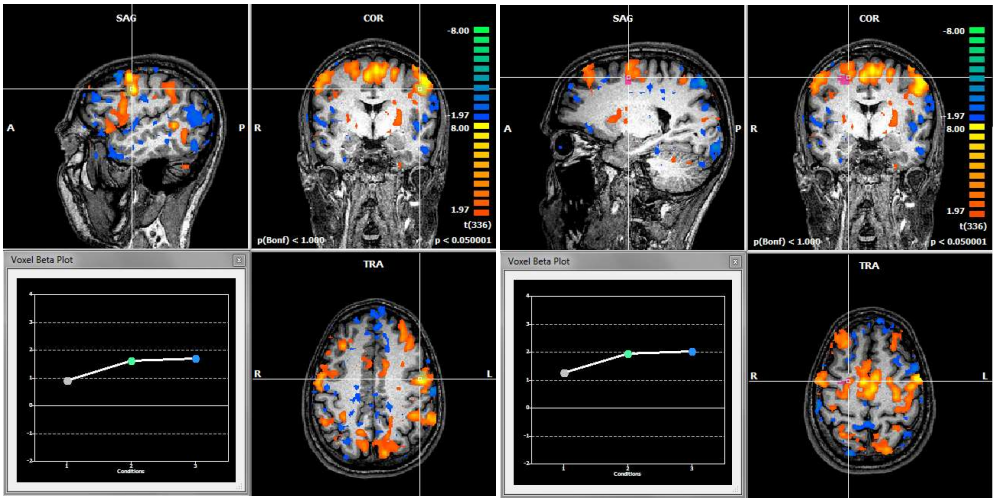

Figure 23. Second Pilot Localizer run activation map with p<0.05 and contrast MI greater than Baseline with the overlap of the ROIs selected online through TBV (on the left the lPMC and on the right the rPMC). Also present the plot of their Beta regression coefficients activation in the three conditions - Baseline (gray), Motor Imagery (green) and Motor Performance (blue).

Table 6. Voxel size and position of the ROIs selected online in the Localizer run.

Region of Interest	Voxels	Talairach coordinates (x,y,z)
lPMC	1018	(-49, -2, 39)
rPMC	447	(25, -6, 50)

Imagery runs

The result of the normality test (**Annex III**) show that not all of correlation values follow a normal distribution, and as a consequence, non-parametric tests will be performed, as in the First Pilot.

As a reminder, as explained in **Section 4.3,** conditions are **Bimanual condition** where the reference task is the bimanual motor imagery movement, **Unimanual condition** where the reference task is the unimanual imaginary movement and **Baseline**.

Neurofeedback runs

As explained in the **Section 4.3**, two different strategies were used with the main goal of maximizing correlation differences between conditions. The results of the **Wilcoxon test** performed for each condition and each one of the three NF runs are in the **Table 7** and the median values of each condition for each NF run are listed in **Table 8.**

Table 7. Wilcoxon Mann-Whitney test comparing correlation distributions from the three conditions present, in the three NF runs, with statistical significance of 0.05.

	Bimanual-Baseline			Unimanual-Baseline			Bimanual-Unimanual		
Run \ Condition	p	h	stats	p	h	stats	p	h	stats
NF run 1	7,35E-01	0	3,39E-01	1,47E-01	0	1,45E+00	4,52E-01	0	-7,52E-01
NF run 2	1,72E-01	0	1,37E+00	6,07E-03	1	2,74E+00	2,67E-01	0	-1,11E+00
NF run 3	4,35E-01	0	-7,80E-01	5,29E-01	0	6,30E-01	5,47E-01	0	-6,02E-01

Table 8. Median values for the correlation distribution for the three conditions in the three NF runs.

	Median		
Run \ Condition	Bimanual	Unimanual	Baseline
NF run 1	0,14	0,13	0,03
NF run 2	0,07	0,16	0,05
NF run 3	0,12	0,21	0,07

The correlation values were relatively low, considering correlation median values. The null hypothesis was only rejected in one neurofeedback run with the first strategy being used, having no correlation statistically different using the second strategy for varying BOLD signal. The plot of the distributions is present in **Figure 24**.

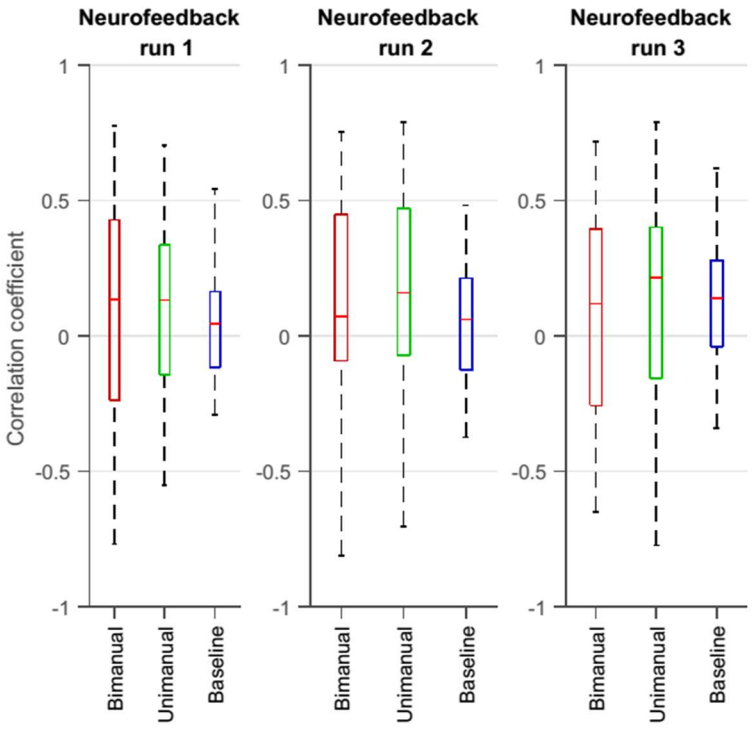

Figure 24. Correlation distribution between conditions in the three NF runs of the second pilot.

For understanding the effect of the strategies used in the ROIs activation, we investigated the ERA of the NF runs.

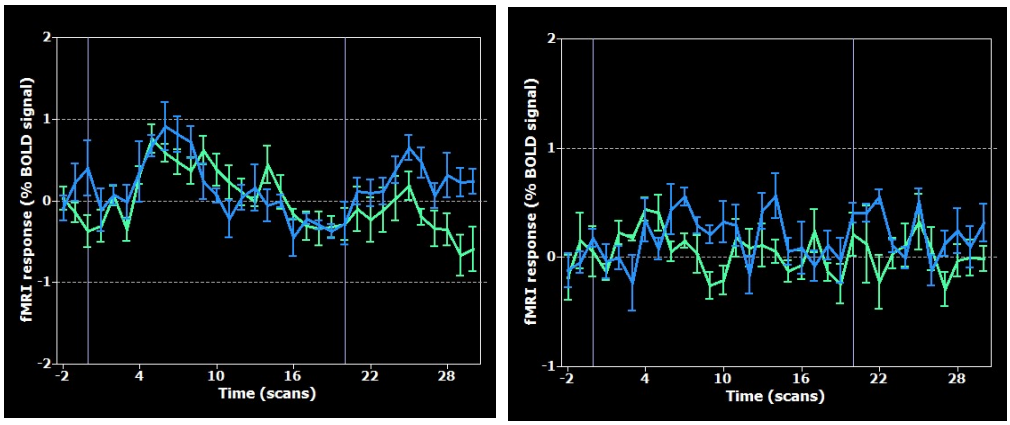

Figure 25. ERA of the first two NF runs in the lPMC (on the left) and in the rPMC (on the right). The green curve represents ERA of condition **Bimanual** and blue represents ERA of condition **Unimanual.**

In the first two neurofeedback runs, it is visible in **Figure 25**, a variation of the lPMC BOLD signal during the duration of the block, with an initial increase followed by a gradual descent until the 20 point block, in both **Bimanual** and **Unimanual** conditions with a **triangular shape** as pretended. In the rPMC, this behavior is not very well defined, although such behavior is noted in the **Unimanual** condition.

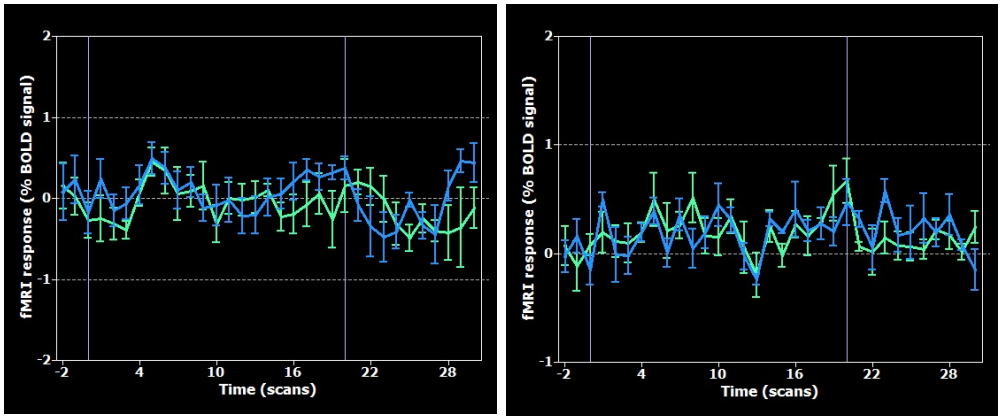

Figure 26. ERA of the third NF runs in the lPMC (on the left) and in the rPMC (on the right). *The green curve represents ERA of condition **Bimanual** and blue represents ERA of condition **Unimanual.***

In the ERA of the third NF run, **Figure 26,** lPMC BOLD variation throughout the duration of the block is not verified for both **Bimanual** and **Unimanual** conditions. In the rPMC, the amplitude of the BOLD variation is close to zero, since it appears that it is mostly noise.

Shortcomings

Correlation values were low comparing with the first pilot study. Activation patterns in rPMC were not as expected, since the triangular shape was not as prominent as in the lPMC. However, the first strategy presented better results and better feedback by the participant.

5.1.3. Third Pilot

Both this and the next Pilots (**Section 5.1.4**) were used to validate the findings of the previous Pilot. As explained in **Section 4.3** the main goal of these pilots was to validate the strategy with better results in the second pilot as to differentiate correlation distributions between conditions.

Localizer run

Confirmation of the online selected ROI is highlighted in **Figure 27**, presenting a correct overlay between both and an activated voxels in the GLM. There is a larger number of active voxels corresponding to the lPMC, which corresponds to the subject's dominant motor hemisphere (the participant was right-handed), also visible in **Table 9**.

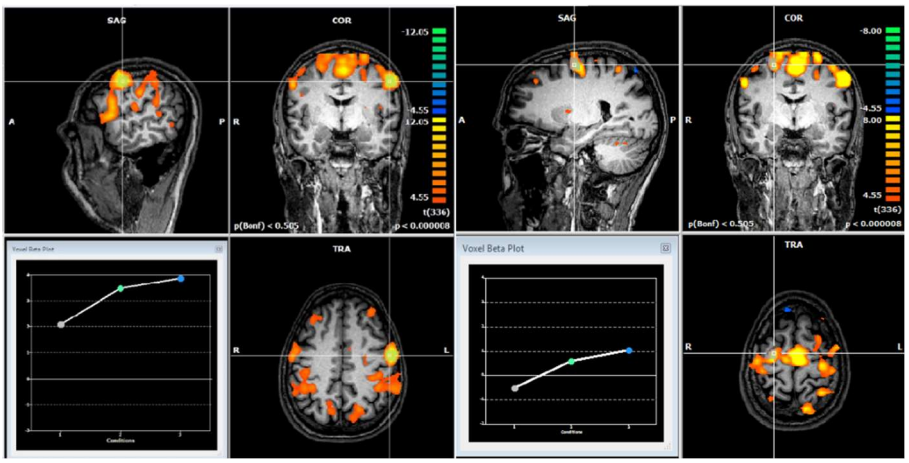

Figure 27. Third Pilot Localizer runs' activation map from with p<0.0000008 and contrast MI greater than Baseline with the overlap of the ROIs selected online through TBV (on the left the IPMC and o the right the rPMC). There is also the plot of their Beta regression coefficients activation in the three conditions – Baseline (gray), Motor Imagery (green), and Motor Performance (blue).

Table 9. Voxel size and position of the ROIs selected online in the Localizer run.

Region of Interest	Voxels	Talairach coordinates (x,y,z)
lPMC	1866	(-55 , 7, 45)
rPMC	1490	(26, -9, 64)

Imagery runs

The result of the normality test (**Annex III**) shows that most of correlation values do not follow a normal distribution, and as a consequence, non-parametric tests will be performed, such as in the previous pilots. As a reminder, as explained in **Section 4.3**, conditions are **Bimanual condition** where

the reference task is the bimanual motor imagery movement, **Unimanual condition,** where the reference task is the unimanual imaginary movement and **Baseline.**

Neurofeedback runs

The results of the **Wilcoxon test** for the three NF runs are in the **Table 10**, with the medians of each condition represented in **Table 11.**

Table 10. Wilcoxon Mann-Whitney test comparing correlation distributions from the three conditions present, in the three NF runs, with statistical significance of 0.05.

	Bimanual-Baseline			Unimanual-Baseline			Bimanual-Unimanual		
Run \ Condition	**p**	**h**	**stats**	**p**	**h**	**stats**	**p**	**h**	**stats**
NF run 1	3,27E-04	1	3,59E+00	5,36E-06	1	4,55E+00	4,46E-01	0	-7,63E-01
NF run 2	1,18E-06	1	4,86E+00	5,00E-10	1	6,22E+00	8,09E-02	0	-1,75E+00
NF run 3	1,62E-01	0	1,40E+00	4,82E-02	1	-1,98E+00	8,90E-03	1	2,62E+00

Table 11. Median values for the correlation distribution for the three conditions in the three NF runs.

	Median		
Run \ Condition	**Bimanual**	**Unimanual**	**Baseline**
NF run 1	0,65	0,71	0,57
NF run 2	0,59	0,62	0,31
NF run 3	0,44	0,23	0,38

The correlation values were considerably high (compared to the previous pilot studies), as showed in **Table 10** and **Table 11** shows a statistical significant difference between the conditions **Bimanual** and **Baseline** in all three NF runs, being the condition **Bimanual** the one with higher values of correlation between them. This difference is present also in conditions **Bimanual** and **Unimanual**, although in the first two NF runs the condition **Unimanual** has a higher correlation value, as visible in **Figure 28**.

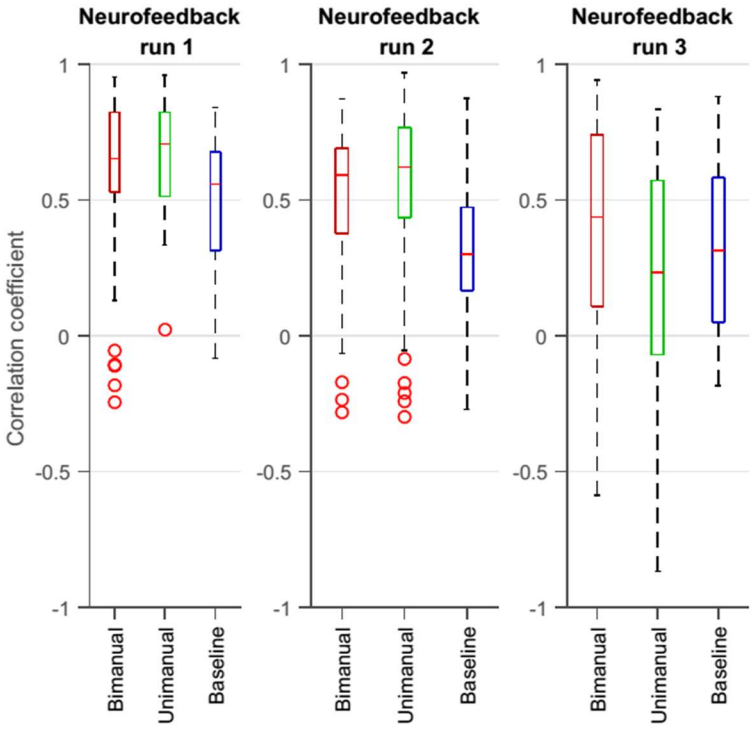

Figure 28. Correlation distribution between conditions in the three NF runs of the third pilot.

To validate the strategy in terms of BOLD signal, the **Figure 29** represents the ERA for all three NF runs.

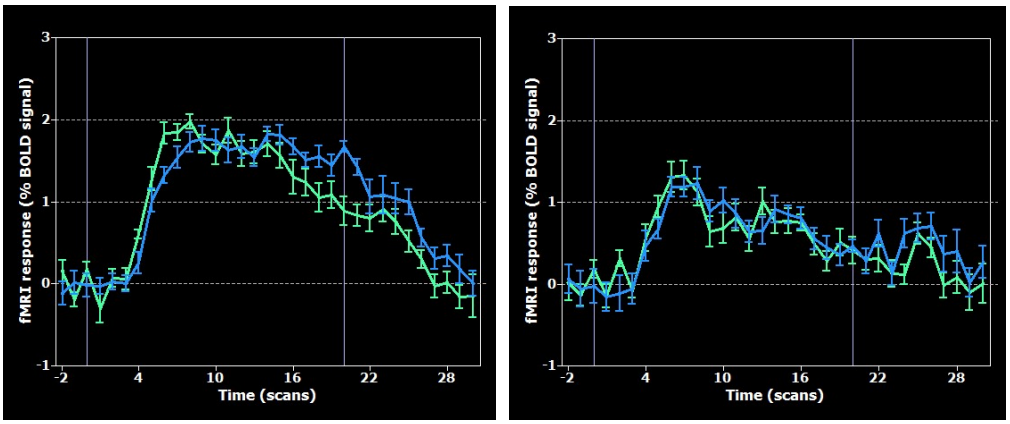

Figure 29. ERA of all the three NF runs in the lPMC (on the left) and in the rPMC (on the right). The green curve represents ERA of condition **Bimanual** and blue represents ERA of condition **Unimanual.**

This high correlations can be explained by **Figure 29**. During all three neurofeedback runs, in both PMC, there was a variation of the BOLD signal within condition **Bimanual** and also in the **Unimanual** block, with an initial increase followed by a gradual descent. This **triangular shape** ERA plot was more prominent in the dominant motor hemisphere, in the lPMC. However, in rPMC, BOLD signal reach closer values to zero at the end of the block.

Training and Transfer runs

The results of the **Wilcoxon test** performed to determine if correlation distributions are significantly different in both Training and Transfer run are in the **Table 12** with the medians presented in **Table 13**.

Table 12. Wilcoxon Mann-Whitney test comparing correlation distributions from the three conditions present, in both Training and Transfer runs, with statistical significance of 0.05.

	Bimanual-Baseline			**Unimanual-Baseline**			**Bimanual-Unimanual**		
Run \ Condition	**p**	**h**	**stats**	**p**	**h**	**stats**	**p**	**h**	**stats**
Training	1,92E-02	1	2,34E+00	3,48E-04	1	3,58E+00	7,76E-01	0	-2,85E-01
Transfer	2,80E-02	1	2,20E+00	3,05E-01	0	-1,02E+00	6,43E-03	1	2,72E+00

Table 13. Median values for the correlation distribution for the three conditions in both Training and Transfer runs.

	Median		
Run \ Condition	**Bimanual**	**Unimanual**	**Baseline**
Training	0,49	0,58	0,34
Transfer	0,48	0,35	0,32

Wilcoxon Mann-Whitney test allowed to reject the null hypothesis in both runs only comparing **Bimanual** and **Baseline** conditions with correlation values higher for the first conditions and lower for the second, as visible in **Figure 30**.

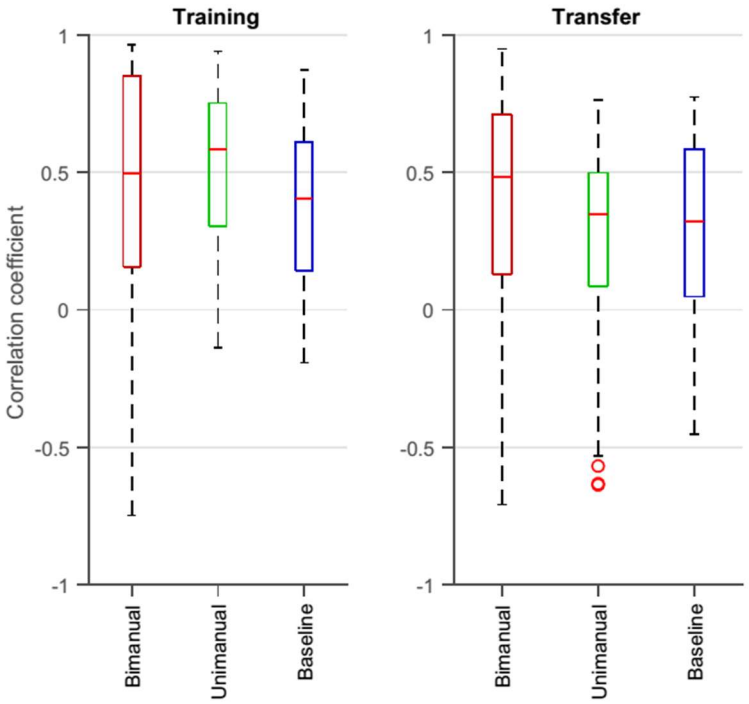

Figure 30. Correlation distribution between conditions for both Training and Transfer runs of the third pilot.

In terms of activation in the Training run, both ROIs BOLD variation was similar to the NF runs, but with the final decrease in BOLD signal not so prominent, **Figure 31**.

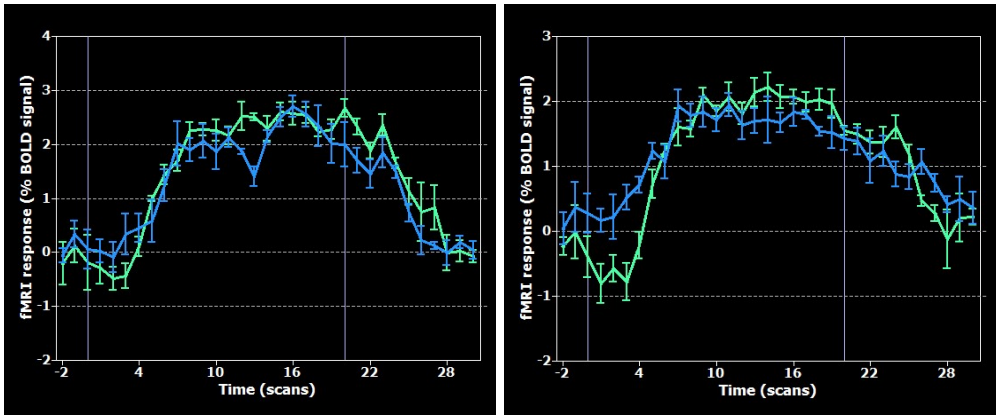

Figure 31. ERA of the Training run in the lPMC (on the left) and in the rPMC (on the right). *The green curve represents ERA of condition **Bimanual** and blue represents ERA of condition **Unimanual.***

This decrease of the BOLD signal is best noted in Transfer run, in both lPMC conditions and in the condition **Bimanual** in the rPMC. However, in lPMC the gradual decrease is not enough to BOLD signal achieve the value of zero at the end of the 20 point block, **Figure 32**.

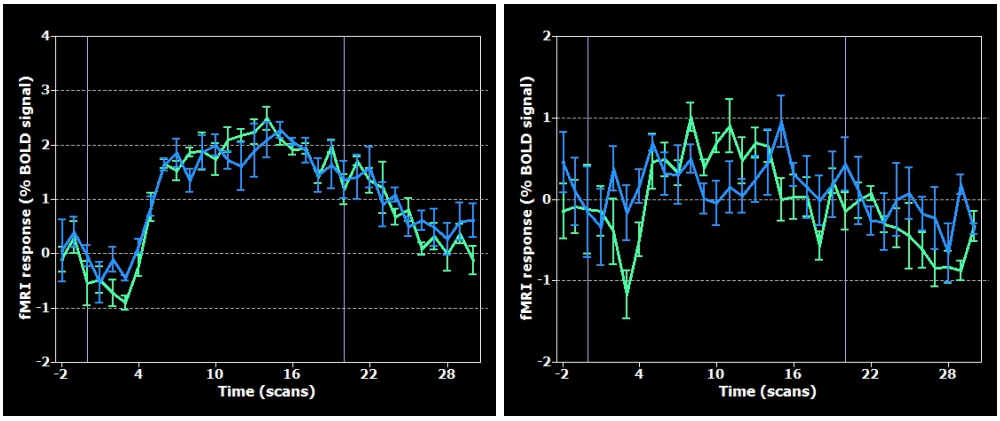

Figure 32. ERA of the Transfer run in the lPMC (on the left) and in the rPMC (on the right). The green curve represents ERA of condition **Bimanual** and blue represents ERA of condition **Unimanual.**

5.1.4. Fourth Pilot

Localizer run

Correct correspondence of online selected ROIs and the offline activation map is highlighted in **Figure 33**. There is a larger number of active voxels corresponding to the rPMC, which does not correspond to the subject's dominant motor hemisphere, visible in **Table 14**.

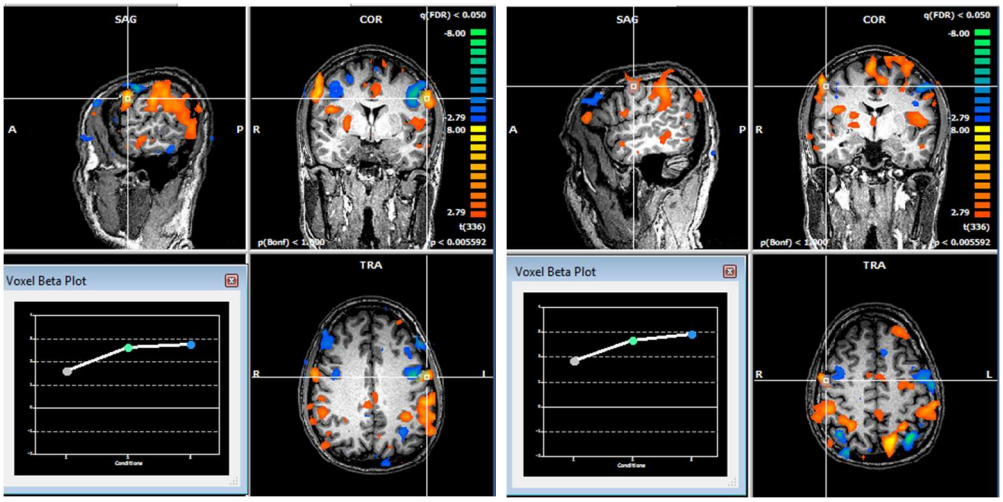

Figure 33. Fourth Pilot Localizer runs' activation map with p<0.05 and contrast MI greater than Baseline with the overlap of the ROIs selected online through TBV (on the left the lPMC and on the right the rPMC). It is also represented the plot of their Beta regression coefficients activation in the three conditions - Baseline (gray), Motor Imagery (green) and Motor Performance (blue).

Table 14. Voxel size and position of the ROIs selected online in the Localizer run.

Region of Interest	Voxels	Position(x,y,z)
lPMC	841	(-55, -2, 33)
rPMC	1087	(50, -6, 45)

Imagery runs

Has it happened with the previous pilots, not all correlation distributions follow the same behavior. In this case the majority of correlations do not follow a normal distribution, hence the use of non-parametric statistical tests (**Annex III**). As a reminder, as explained in **Section 4.3,** conditions are **Bimanual condition** where the reference task is the bimanual motor imagery movement, **Unimaual condition** where the reference task is the unimanual imaginary movement and **Baseline.**

Neurofeedback runs

The results of the **Wilcoxon test** performed for all three NF runs **Table 15** with the medians presented in **Table 16.**

Table 15. Wilcoxon Mann-Whitney test comparing correlation distributions from the three conditions present, in the three NF runs, with statistical significance of 0.05.

	Bimanual-Baseline			Unimanual-Baseline			Bimanual-Unimanual		
Run \ Condition	p	h	stats	p	h	stats	p	h	stats
NF run 1	5,96E-01	0	5,30E-01	7,92E-02	0	-1,76E+00	6,12E-02	0	1,87E+00
NF run 2	5,24E-03	1	2,79E+00	1,16E-04	1	3,86E+00	1,18E-01	0	-1,56E+00
NF run 3	2,76E-06	1	-4,69E+00	5,93E-01	0	-5,35E-01	8,10E-04	1	-3,35E+00

Table 16. Median values for the correlation distribution for the three conditions in the three neurofeedback runs.

	Median		
Run \ Condition	Bimanual	Unimanual	Baseline
NF run 1	0,53	0,30	0,47
NF run 2	0,68	0,73	0,52
NF run 3	0,30	0,52	0,59

In two NF runs, distribution correlations of conditions **Bimanual** and **Baseline** were considered statistically different although in one NF run, condition **Baseline** correlation values were higher. Comparing other conditions, in only one NF, correlation distributions were significantly different, as also visible in **Figure 34**.

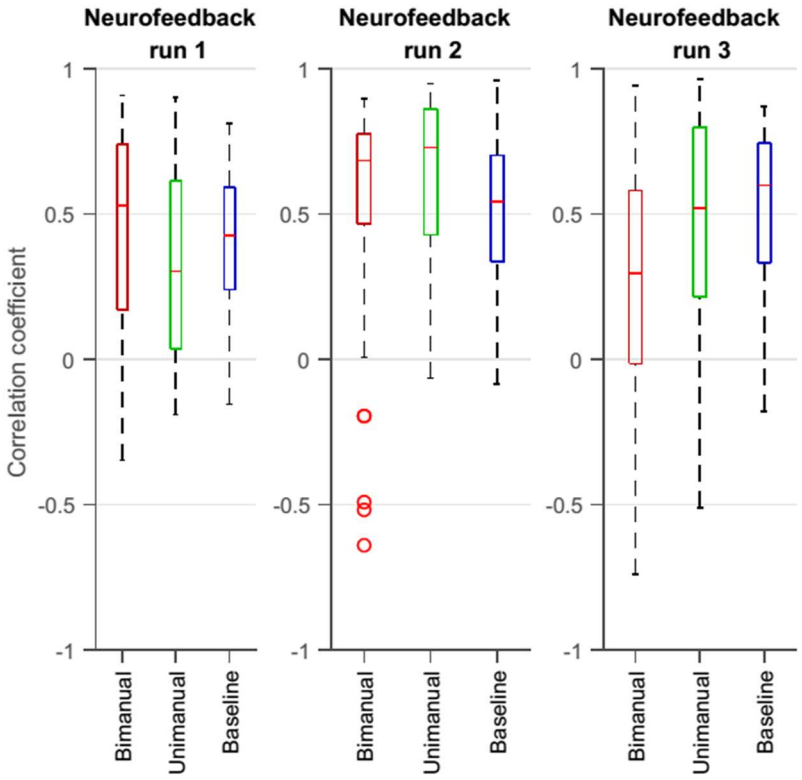

Figure 34. Correlation distribution between conditions for all three NF runs of the fourth pilot.

In the ERA plot of the three NF runs, **Figure 35**, there is a similar shape for both premotor areas, with an increase until the 10 point mark followed by a decrease of the BOLD variation close to zero in condition **Bimanual**. This goes along with the expected results. However, this similarity in both PMC activation is also present in condition **Unimanual.** The amplitude of the variations were significantly bigger in the rPMC, corresponding to the hand (left-hand) as the participant used for reference for unimanual imagined movements.

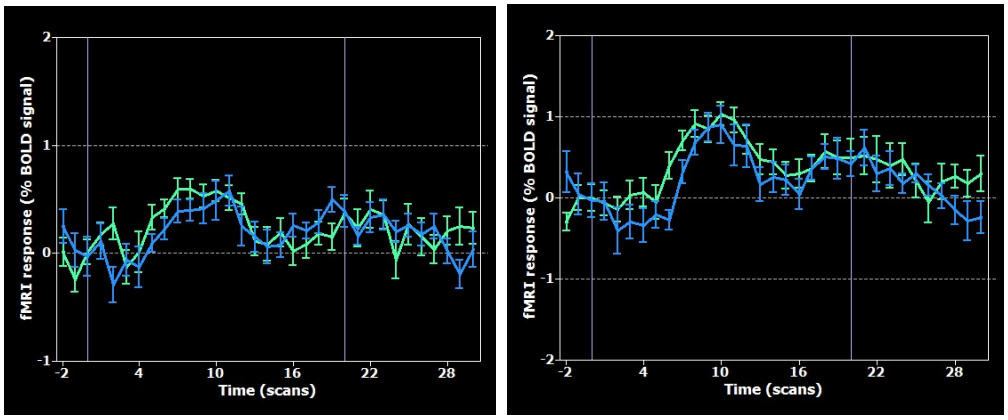

Figure 35. ERA of the three NF runs in the lPMC (on the left) and in the rPMC (on the right). The green curve represents ERA of condition **Bimanual.** and blue represents ERA of condition **Unimanual.**

Training and Transfer runs

The results of the **Wilcoxon test** performed to determine if correlation distributions are significantly different in both Training and Transfer run are in the **Table 17** with the medians presented in **Table 18**.

Table 17. Wilcoxon Mann-Whitney test comparing correlation distributions from the three conditions present, in both Training and Tranfers, with statistical significance of 0.05.

	Bimanual-Baseline			Unimanual-Baseline			Bimanual-Unimanual		
Run \ Condition	p	h	stats	p	h	stats	p	h	stats
Training	4,47E-08	1	5,47E+00	2,52E-02	1	2,24E+00	2,12E-02	1	2,31E+00
Transfer	3,54E-02	1	2,10E+00	2,23E-11	1	6,69E+00	4,29E-07	1	-5,06E+00

Table 18. Median values for the correlation distribution for the three conditions in both Training and Transfer runs.

	Median		
Run \ Condition	Bimanual	Unimanual	Baseline
Training	0,60	0,48	0,35
Transfer	0,60	0,79	0,40

The null hypothesis was rejected in both runs for all the three conditions, **Table 17**, with **Bimanual** and **Unimanual** correlation values higher than **Baseline**. However, the condition with highest correlation values alternates between **Bimanual** and **Unimanual** for both runs, as visible in **Figure 36**.

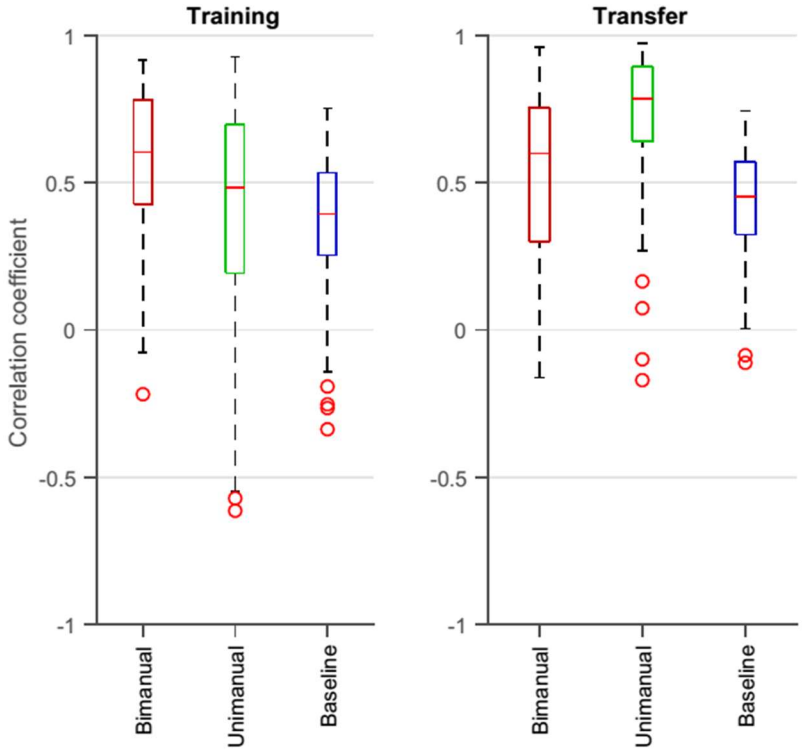

Figure 36. Correlation distribution between conditions for both Training and Transfer runs of the fourth pilot.

Regarding the Training run, the increased and consequent decrease of the variation of BOLD is more noticeable in the lPMC, in condition **Unimanual**, **Figure 37.**

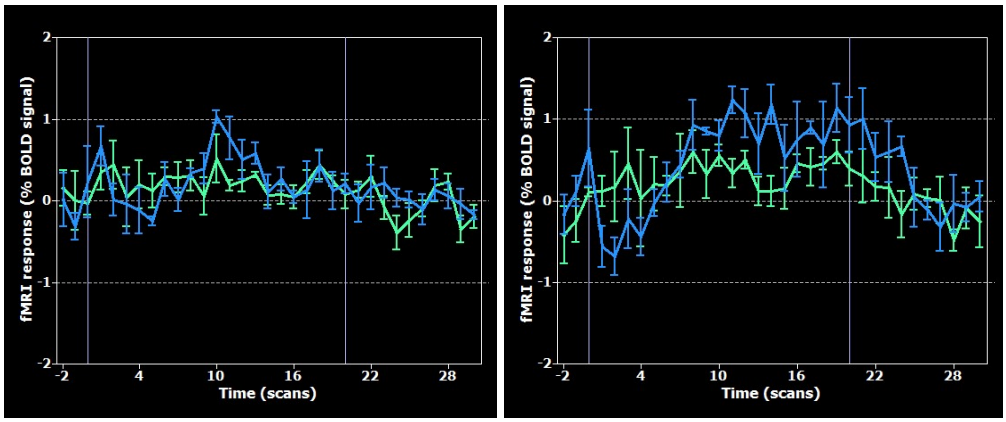

Figure 37. ERA of the Training run in the lPMC (on the left) and in the rPMC (on the right). The green curve represents ERA of condition **Bimanual** and blue represents ERA of condition **Unimanual.**

In terms of the Transfer run, in both premotor areas the curves seem more well defined, although it is visible the lack of decreasing BOLD variation in the second half of the 20 point block for condition **Unimanual**, **Figure 38**.

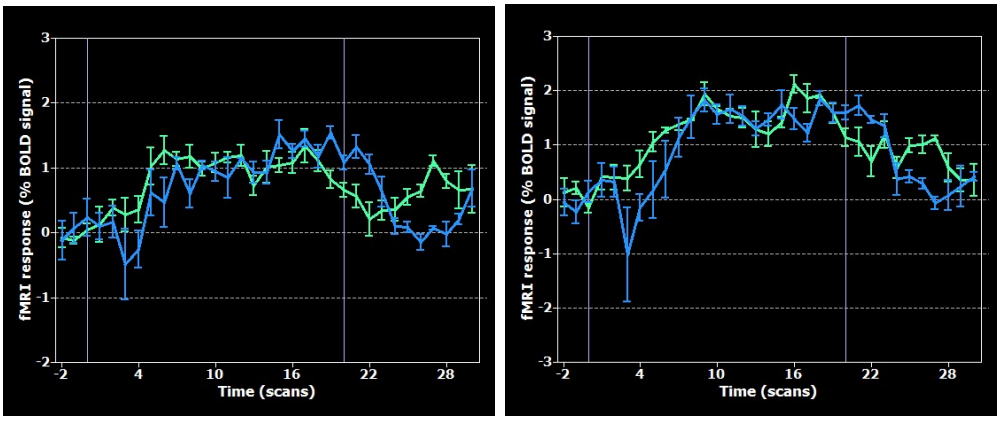

Figure 38. ERA of the Transfer run in the lPMC (on the left) and in the rPMC (on the right). The green curve represents ERA of condition **Bimanual** and blue represents ERA of condition **Unimanual.**

Shortcomings and Final Protocol

Condition **Unimanual** activation pattern was not as expected, with reported activation in both PMC. As consequence, correlation values were high, with correlation distributions significantly different from condition **Baseline** in several cases.

As consequence, the decision was made to remove this condition **Unimanual** making the commitment with two conditions: up-regulation and a down-regulation of functional connectivity between bilateral PMC.

5.2. Final Experiment

We proceeded to the rt-fMRI-NF acquisition of 10 healthy participants (see **Section 4.1**) with the final protocol optimized, with imagery runs with only two conditions: **i. *Increase*** *connectivity blocks where the reference task is the bimanual motor imagery movement*, **ii. *Decrease*** *connectivity blocks in which the subjects were asked to decrease the feedback by not activating premotor cortex areas* (as described in **Section 4.2.2**).

5.2.1. Localizer run

Table 19. Localization in Talairach coordinates of the online selected ROIs, the lPMC and rPMC, with the contrast MI>Baseline. The size of the ROIs was according to the default threshold (3.0) in TBV and each ROI was selected using a single click. Subject 4 (*) lPMC ROI was selected with threshold value of 2.4.

Subject	Voxels lPMC	TAL coordinates (x,y,z)	Voxels rPMC	TAL coordinates (x,y,z)
Subject 1	2117	(-46, -7, 52)	1472	(46, -5, 56)
Subject 2	900	(-51, 6, 43)	950	(48, -1, 51)
Subject 3	546	(-50, -4, 46)	653	(53, -6, 39)
Subject 4	1076*	(-60, 3, 39)	460	(46,-7,46)
Subject 5	382	(-61, -3, 40)	620	(47, -7, 48)
Subject 6	819	(-34, -15, 54)	502	(37, -15, 50)
Subject 7	377	(-21, -11, 52)	771	(30, -15, 55)
Subject 8	1203	(-39, -11, 48)	1009	(42, -8, 48)
Subject 9	811	(-26, -4, 43)	260	(48, -3, 40)
Subject 10	546	(-58, 5, 39)	542	(28, -1, 65)

The variability of the location of PMC areas activated as well as the number of voxels activated is denoted in the previous **Table 19**.

Taking this into account, and according to the **Section 4.4** the multi-subject analysis proposed was the RFX group analysis. **Figure 39** and **40** represent the activation map using Random Effects (RFX) group analysis.

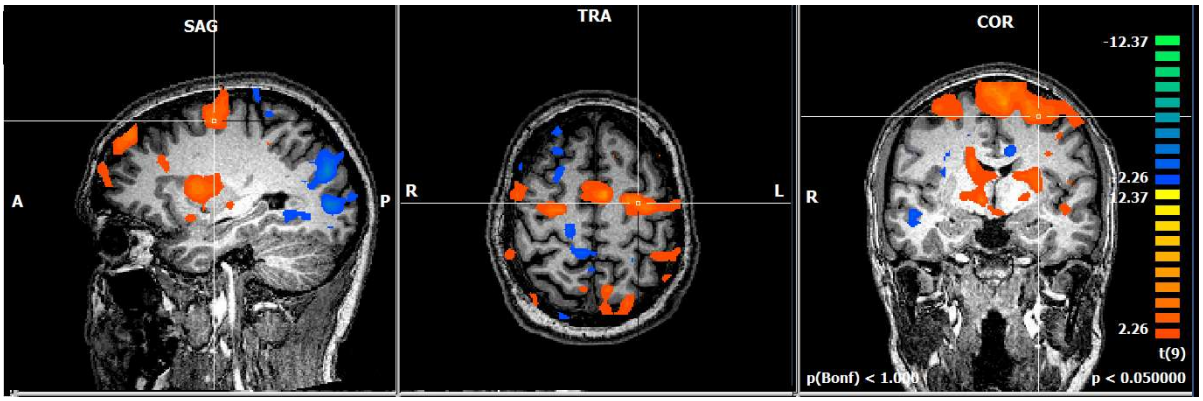

Figure 39. Multi Subject GLM activation map, MI> Baseline, p<0.05, left hemisphere.

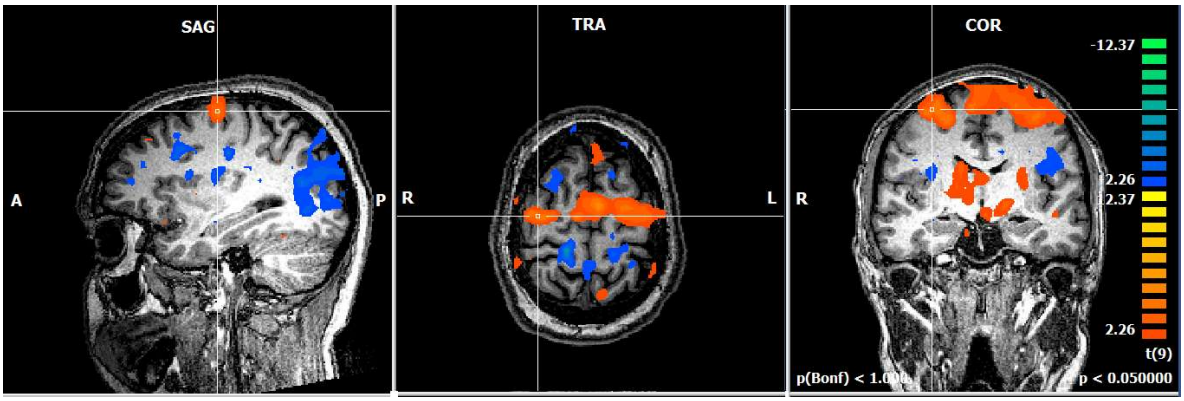

Figure 40. Multi Subject GLM activation map, MI> Baseline, p<0.05, right hemisphere.

The group statistical maps of the localizer run is presented in **Figure 39** and **Figure 40**.They show the areas activated during the Localizer run, with contrast MI greater than Baseline, using one of the subjects structural brain image as anatomical reference .

It is visible that motor areas and premotor areas, anterior to M1, located in an anterior portion of the central sulcus are statistically active. There is also, as expected, an activation in a medial area that corresponds to the SMA. There is a visible larger activated area in the left hemisphere, congruent with the **Table 19**.

5.2.2. Neurofeedback runs

With the normal behavior of the distributions of correlations not guaranteed for all runs and subjects, as it happened previously, non-parametric tests were performed and medians were used as a central tendency measure.

Is important to verify which brain areas are more active between conditions in all NF runs. According to the **Section 4.4** the multi-subject analysis proposed was the RFX group analysis. **Figure 41** and **42** represent the activation map using RFX group analysis of all three NF runs by all the 10 subjects, with contrast **i.Increase>ii.Decrease**.

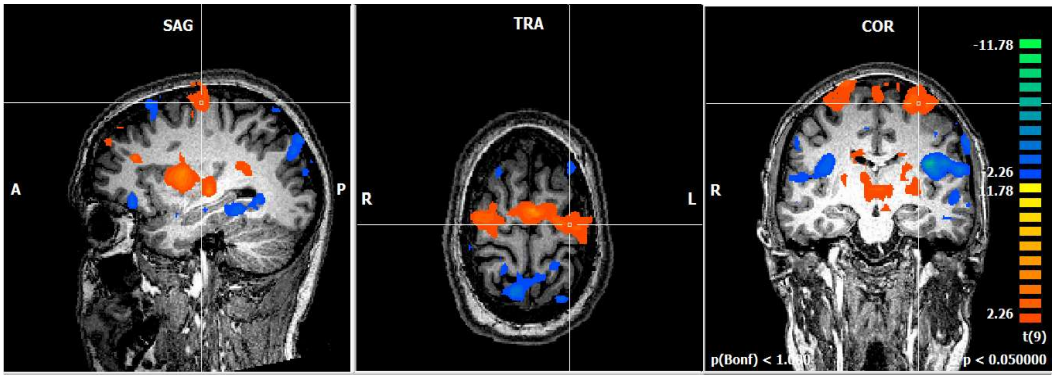

Figure 41. Multi Subject GLM activation map, **i.Increase>ii.Decrease** , p<0.05, lPMC.

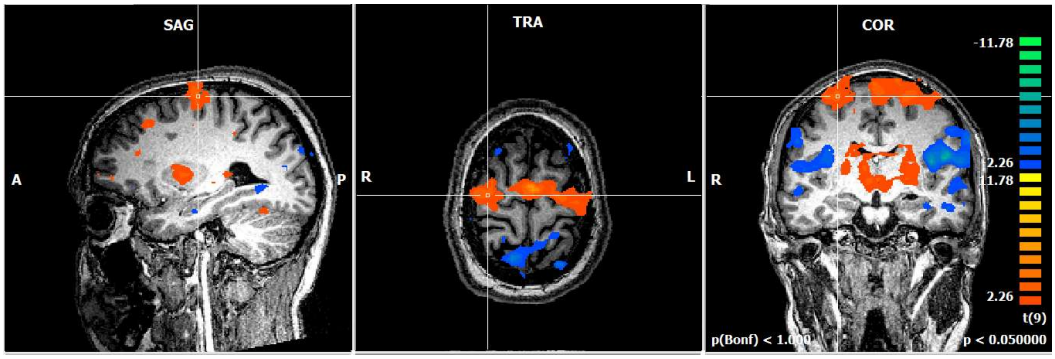

Figure 42. Multi Subject GLM activation map, **i.Increase.>ii.Decrease** , p<0.05, rPMC.

The active areas in NF runs, with statistical significance of 0.05, have a resemblance with the Localizer run activation map, regarding the non-primary motor cortex i.e., there are activations in

regions anterior to the M1, the PMC and also a medial area, the SMA. This RFX analysis is a valid confirmation of the success of the Localizer run task.

Regarding the NF runs performed by all ten subjects, the medians correlation values for each condition are listed in the **Table 20**, is possible to verify a large range of results, having subjects that tend to have high correlation values and other subjects that show low correlation values all along the session.

Table 20. Median values for the correlation distribution for the two conditions i - decrease connectivity, ii-increase connectivity in the three neurofeedback runs for all the 10 subjects.

	Median					
	Neurofeedback run 1		Neurofeedback run 2		Neurofeedback run 3	
Subject	i.Increase	ii.Decrease	i.Increase	ii.Decrease	i.Increase	ii.Decrease
Subject 1	0.55	0.61	0.54	0.57	0.45	0.59
Subject 2	0.67	0.53	0.62	0.36	0.38	0.66
Subject 3	0.47	0.66	0.49	0.60	0.64	0.52
Subject 4	0.41	0.53	0.40	0.26	0.44	0.56
Subject 5	0.59	0.44	0.37	0.46	0.39	0.45
Subject 6	0.33	0.27	0.45	0.38	0.17	0.32
Subject 7	0.46	0.33	0.40	0.42	0.27	0.37
Subject 8	0.58	0.80	0.55	0.66	0.58	0.69
Subject 9	0.43	0.49	0.51	0.35	0.39	0.48
Subject 10	0.07	0.22	0.24	0.07	0.15	0.27

In terms of distribution of correlation difference between the condition **i.Increase** and **ii.Decrease**, for all three NF runs performed by the 10 subjects, the results of the **Wilcoxon Mann-Whitney test** are listed in the **Table 21**.

Table 21. Wilcoxon Mann-Whitney test comparing correlation distributions from both conditions present, in the three NF runs, with statistical significance of 0.05. The runs with (*) are the ones in which **i.Increase** correlation values are higher than **ii.Decrease.**

	p-val			h			z-value		
Subject	NF1	NF2	NF3	NF1	NF2	NF3	NF1	NF2	NF3
Subject 1	1,84E-02	4,18E-01	2,10E-03	1	0	1	-2,36	-0,81	-3,08
Subject 2	3,52E-07	3,03E-07	9,21E-07	1*	1*	1	5,09	5,12	-4,91
Subject 3	2,95E-08	1,72E-06	1,45E-02	1	1	1*	-3.26	-3.83	4.07
Subject 4	7,19E-04	1,07E-02	5,07E-03	1	1*	1	-3,38	2,55	-2,80
Subject 5	6,88E-03	2,05E-02	3,77E-02	1*	1	1	2,70	-2,32	-2,08

Subject 6	1,87E-01	2,35E-02	3,70E-03	0	1*	1	1,32	2,27	-2,90
Subject 7	2,65E-02	4,89E-01	2,70E-02	1*	0	1	2,22	0,69	-2,21
Subject 8	6,95E-10	6,25E-04	1,57E-02	1	1	1	-6,17	-3,42	-2,42
Subject 9	4,34E-01	1,42E-04	9,31E-01	0	1*	0	-0,78	3,81	-0,09
Subject 10	1,36E-02	4,97E-04	9,94E-02	1	1*	0	-2,47	3,48	-1,65

From the ten subjects, eight were able to self-modulate their functional connectivity between bilateral PMC in at least one neurofeedback run. From those eight, only one was able to correct self-modulate in two distinct neurofeedback runs.

In a total of 30 NF run (three per subject), nine runs presented higher correlation values in condition **i.Increase** comparing to **ii.Decrease** However, 24 out of 30 runs showed a statistical difference in correlations values between conditions, meaning that the correlation values in condition **ii.Decrease** were higher than in condition **i.Increase** in 15 NF runs.

The NF run with the more expected distribution of correlations was NF run 2, with five out of 10 runs with successful self-modulation. On the other hand, NF run 3 was the one with worst results, with one corrected self-modulation run and with seven runs with higher correlation in condition **ii.Decrease**.

Debriefing analysis

Another very important type of results is the response of the questionnaires by the subjects who participated in the experiment (**Annex II**). Eight out of 10 subjects felt like they were in the control of their own PMC connectivity at least in some period in time during the session. From these eight subjects, one of them was not able to correctly self-regulate bilateral premotor connectivity in any run. From the eight subjects that successfully modulated at least one NF run, only *Subject 6* did not feel as if he was controlling the feedback values at some point during the session. Even from the subjects who felt able to self-modulate bilateral PMC, three of them reported greater difficulty and a lesser sense of control in condition **ii.Decrease**.

In order to understand this added difficulty in the condition **ii.Decrease** blocks it was verified how mean correlation values vary within condition blocks. The following correlation ERA (**Figure 43** through **47**) plots are from the NF runs from the subjects that self-modulated their functional connectivity with higher correlation in **ii.Decrease** or at least had a very delayed self-correlation in two NF runs.

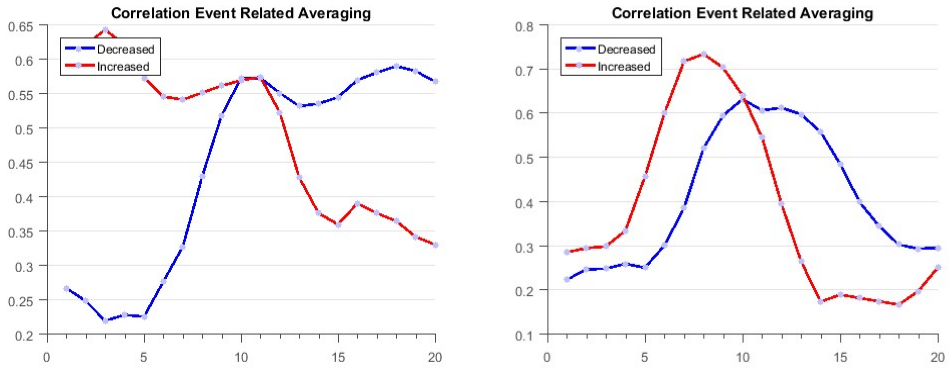

Figure 43. Subject 1, NF1 and NF3 correlation ERA, 20 point block

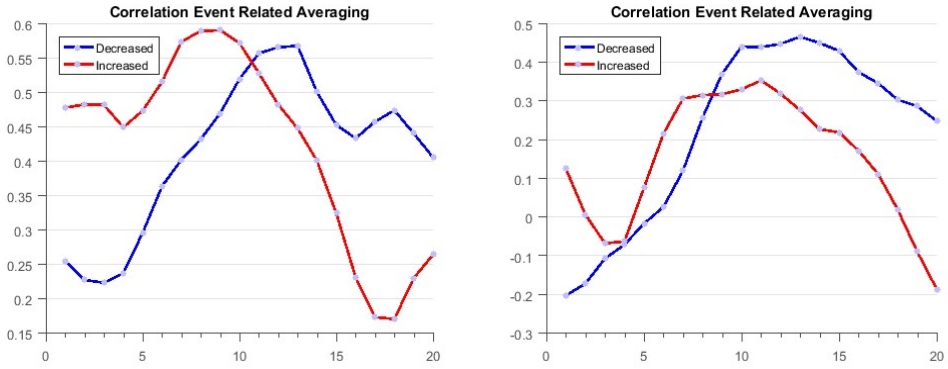

Figure 44. Subject 3, NF1 and NF2 correlation ERA, 20 point block.

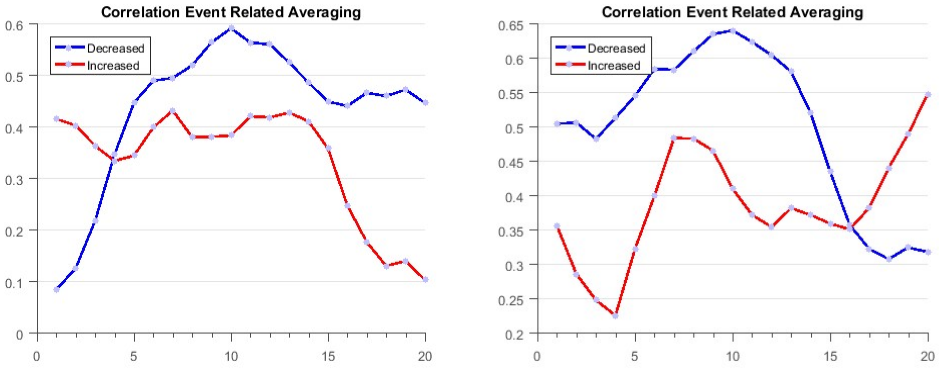

Figure 45. Subject 4, NF1 and NF3 correlation ERA, 20 point block.

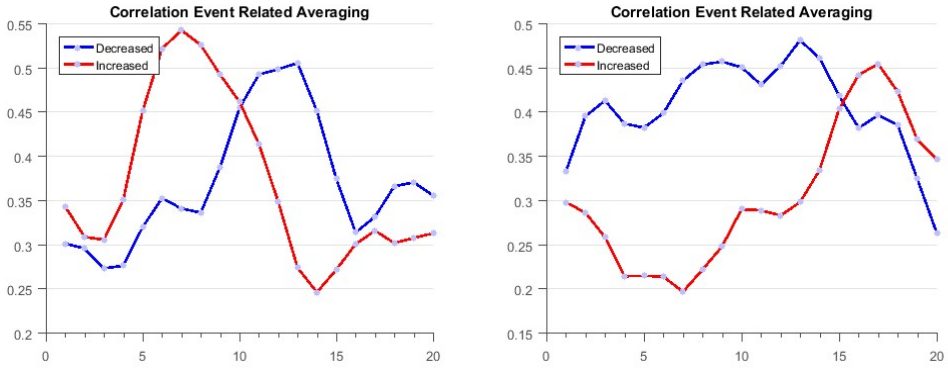

Figure 46 .Subject 5, NF2 and NF3 correlation ERA, 20 point block.

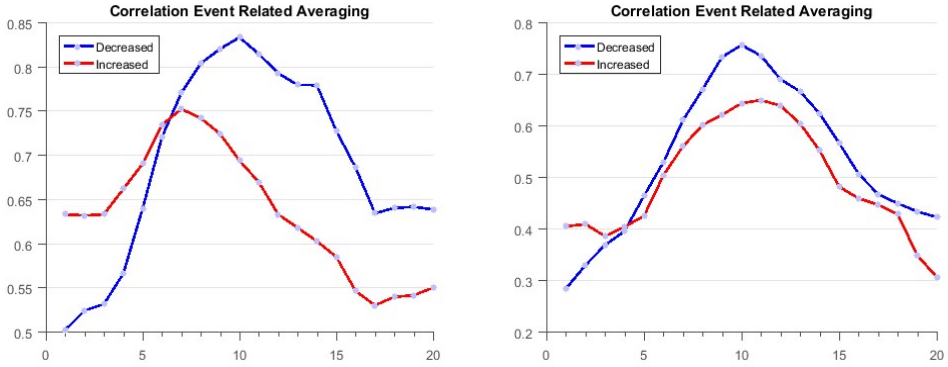

Figure 47. Subject 8, NF1 and NF3 correlation ERA, 20 point block.

In terms of correlation ERA, for the most part the curves are in anti-phase, and other have the same behavior throughout the 20 point block, only with higher correlation values in the condition **ii.Decrease**.

5.2.3. Training and Transfer runs

With the normal behavior of the distributions of correlations not guaranteed for all runs and subjects, as it happened previously, non-parametric tests were performed and medians were used as a central tendency measure.

In terms of correlation values in Training and Transfer runs, performed by all ten subjects before and after the NF runs, their median results are highlighted in the next **Table 22**.

Table 22. Median values for the correlation distribution for the condition **i.Increase,** and **ii.Decrease** in the Training and Transfer runs for all the 10 subjects, considering a 12 point block.

	Median			
	Training		Transfer	
Subject	i-Increase	ii-Decrease	i-Increase	ii.Decrease
Subject 1	0,47	0,48	0,53	0,45
Subject 2	0,72	0,47	0,39	0,63
Subject 3	0,41	0,52	0,40	0,39
Subject 4	0,48	0,55	0,47	0,35
Subject 5	0,52	0,47	0,35	0,47
Subject 6	0,30	0,48	0,05	0,40
Subject 7	0,39	0,25	0,40	0,49
Subject 8	0,54	0,67	0,64	0,73
Subject 9	0,37	0,38	0,58	0,35
Subject 10	0,16	0,12	0,45	0,11

In order to find if subjects were able to self-modulate their functional connectivity between ROIs in imagery runs in which feedback was not given, we performed **Wilcoxon Mann-Whitney test**. The results are listed in the **Table 23** below.

Table 23. Wilcoxon Mann-Whitney test, with the null hypothesis that the distribution of the correlation from different conditions in the neurofeedback runs are samples from one continuous distributions with equal medians, against the alternative that they are not with a 0.05 significance level, considering a 12 point block.

	p-val		h		z-value	
Subject	Training	Transfer	Training	Transfer	Training	Transfer
Subject 1	7,97E-01	1,10E-01	0	0	0,26	1,60
Subject 2	7,27E-10	8,97E-05	1*	1	6,16	-3,92
Subject 3	1,17E-01	8,21E-03	0	1	1,57	-2,64
Subject 4	4,82E-02	2,80E-01	1	0	-1,98	1,08
Subject 5	1,68E-01	1,61E-02	0	1	1,38	-2,41
Subject 6	5,39E-05	5,79E-12	1	1	-4,04	-6,88
Subject 7	2,10E-02	1,54E-05	1*	1	2,31	-4,32
Subject 8	8,09E-03	2,46E-05	1	1	-2,65	-4,22
Subject 9	7,69E-01	1,31E-05	0	1*	-0,29	4,36
Subject 10	6,92E-01	4,42E-08	0	1	0,40	-5,47

Possible Skill Learning - Transfer vs Training runs

In between Training and Transfer runs there are three NF runs in which the subject has performed self-modulation of their brain activity. So, it is important to compare the results of this "Pre" and "Post" runs to see a possible effect of NF-training. The approach used was comparing Transfer and Training correlation values for each condition.

Table 24. Wilcoxon Mann-Whitney test for the distribution of the correlation from different runs - Training and Transfer for each condition with a 0.05 significance level.

	p-val		h		z-value	
Subject	**i.Increase**	**ii.Decrease**	**i.**	**ii.**	**i.Increase**	**ii.Decrease**
Subject 1	4,89E-01	5,09E-01	0	0	0,69	-0,66
Subject 2	5,02E-08	2,19E-05	1	1	-5,45	4,24
Subject 3	9,66E-01	8,95E-04	0	1	-0,04	-3,32
Subject 4	3,46E-01	1,66E-05	0	1*	-0,94	-4,31
Subject 5	4,52E-04	7,60E-01	1	0	-3,51	0,31
Subject 6	1,89E-04	9,52E-01	1	0	-3,73	-0,06
Subject 7	4,81E-01	6,62E-11	0	1	-0,71	6,53
Subject 8	4,93E-03	1,62E-03	1*	1	2,81	3,15
Subject 9	2,34E-04	9,37E-01	1*	0	3,68	0,08
Subject 10	2,21E-01	5,87E-08	0	1	-1,22	5,42

In the previous **Table 24** is verifiable a significant increase in correlation values in condition **i.Increase** on two subjects and a decrease in correlation values in condition **ii.Decrease** in one subject, comparing Training and Transfer runs.

Discussion

6.1. Contribution to the State of the Art

Fc-based rt-fMRI-NF is a recent technique, that has proven feasible by Spetter et al. (2017) and Ruiz et al. (2014) work. However, in both of these authors' works, participants were only asked to enhance the functional connectivity between ROIs using contingent rt-fMRI feedback, i.e. no feedback was shown during down-regulation blocks.

PMC had already been used in ROI-based activation NF experiments (Xie et al., 2015). Nevertheless, self-modulation of functional connectivity between both premotor areas as feedback was something, to the best of our knowledge, never done before.

With the previous results, we report a framework that allows subjects to increase and decrease the functional connectivity between bilateral PMC, in the presence of contingent feedback.

6.2. First Pilot

The first Pilot was fundamentally a test to the possibility of an fc-based rt-fMRI-NF experiment using a motor imagery paradigm.

Localizer run

We first had to select online both PMC and to do so, a new functional Localizer run was tested. Although very mentally demanding, it was proven to be a successful one with accurate results since throughout the rest of the functional runs there was a variation in the ROIs BOLD signal with motor imagery tasks.

Imagery runs

The feasibility was proven during the NF runs with lPMC and rPMC activation. In terms of correlation values, condition **Bimanual**, since there was a synchronous PMC activation, presented a

significantly higher than the condition **Baseline** in all three runs. The results of the last neurofeedback run showed a possible idea of three levels of correlation - condition **Bimanual** with the highest values, condition **Baseline** with the lowest correlation values and condition **Unimanual** in between.

However, through the offline analysis, as well as through the participant's debriefing, a conclusion was reached: **a simple activation task** of bilateral premotor is not optimal for PMC self-modulating. This conclusion is made due to the pattern activation of bilateral PMC which has as a consequence low feedback values during part of condition **Bimanual** blocks and an increase in feedback values in the beginning of condition **Baseline** blocks, even though there is no desire or intention of the participant to.

6.3. Second Pilot

To optimize correlation differences between activation conditions, was hypothesized that variations in the BOLD signal throughout the activation blocks would assure a maintenance of high correlation in runs with both PMC activation and feedback values even in the middle of the block, since it was reported as being the most challenging section.

Imagery runs

Comparing the two alternative strategies for maintaining the *variation of the BOLD signal constant* within a block duration, the one used in the first two NF runs seems the most adequate. The formation of **a triangular shape in the ERA plot** in both **Bimanual** and **Unimanual** conditions looks the most promising way to variate gradually the activation of the NF targets, comparing to the ERA plot of the third NF run. This was achieved by variating the frequency of imagined movements - first increasing and after the auditory cue, gradually decreasing the frequency so that at the end of the block, the participant is at resting state.

This conclusion was supported by the feedback given by the participant in the debriefing, confirming the task in which he felt the best able to self-regulate NF was the first, as well as the easiest to perform. Both ROIs selected were confirmed by a trained Neuroradiologist as in fact premotor areas. One of the possible reasons for the low correlation values is based on the position of the ROI (in this

pilot the rPMC was selected more anteriorly). Despite the similar tasks and conditions, the selection online is not trivial and may induce variability.

6.4. Third and Fourth Pilots

Both the third and the fourth pilots were performed in order to confirm and validate the task of varying frequency of imagined movements as the reference task for conditions **Bimanual** and **Unimanual**.

Imagery runs

Regarding the third pilot, it was performed by the same participant who had performed the previous ones. The difference between the ERA of BOLD signal from the NF runs compared to the first pilot is quite remarkable. This means that the participant premeditatedly variated both ROIs activation in the intended way (triangular shape). As a result, correlation values in activation conditions (**Bimanual** and **Unimanual**) were significantly high and **Baseline** correlation values were lowered to the point of the distribution of correlations, in two out of three NF runs, were considered statistically different.

Comparing the ERA of the Transfer Run with the Training Run is possible to see an improvement on the down-regulation in the second half of the activation block of the dominant premotor area (lPMC), after the NF-training.

Regarding the **fourth pilot,** in the NF runs as also able to self-modulate its bilateral premotor activation. In two out of three runs, the median correlation value of the **Bimanual** condition was higher than the **Baseline** one, however in only run the distribution of the correlations was statistically different. In this case, in both **Bimanual** and **Unimanual** conditions the variation of BOLD was significantly higher in the rPMC than in the lPMC, since the subject used left hand imaginary movement as a reference for unimanual tasks.

In the absence of feedback, all distributions were rejected as being part of a continuous distribution with equal medians. The triangular shape of BOLD activation was more present in the

Transfer runs. This suggests a distribution of correlations with **Bimanual** and **Unimanual** conditions with high correlation values and the **Baseline** the lowest.

From the fourth pilot, we can verify that the reference hand for unimanual imagined movements appears to have a higher activation in its contralateral premotor in both **Bimanual** and **Unimanual** conditions, in the NF runs (the participant was right-handed and used the left hand has unimanual reference).

6.5. From testing to the final framework

The **Unimanual** condition, with unimanual imagined tasks, thought to have as consequence a decrease in functional connectivity, has correlation values statistically different from **Baseline** condition in various functional runs. Also, the differentiation of its correlation distribution to the condition **Bimanual** distribution alternates off and on. This, alongside the plots of variation of BOLD signal, shows that in unimanual hand motor tasks there is also an activation of the ipsilateral premotor (to the reference hand) which results in higher correlation values. This activation might be caused by the PMC action, reported by Grefkes et al. (2008), of inhibition of the ipsilateral primary motor cortex (M1), even in motor imagery (MI) tasks.

Having this in mind, a final framework was developed and the functional runs became composed only by two conditions, an up-regulation and a down-regulation blocks, in which the subject is told to increase and decrease their own functional connectivity between bilateral premotor. The reference task for the **increased connectivity** blocks was the imaginary bimanual hand/finger movement and the reference task for the **decrease connectivity** blocks was similar to the previous **Baseline** condition, meaning that the reference task was resting state or another mental task that does not activate premotor areas such as abstract mathematical calculations or N-back calculations, amongst others.

6.6. Multi-Subject Acquisition and Group Analysis

To conclude about the feasibility of NF - connectivity based with a motor imagery paradigm, 10 healthy subjects were recruited, with high scores in MIQ-3 Questionnaire (5,68±0,6 in a 1 to 7 scale) (see **Section 4.1.** and **Annex I**).

It was important to have a heterogeneous population in terms of familiarity with fMRI and rt-fMRI- NF experiments as this is a feasibility test. If this technique is to be used in a clinical population, it is important to know that it works with people independently of their experience in the MRI scanner.

All 10 sessions were performed without any incidents, there was only the need to repeat on the Localizer run, due a mistake between "Motor Imagery" and "Motor Performance" in the early blocks by Subject 5. All subjects perform the experiment as expected, the participant's engagement was satisfactory and were able to finish the rt-fMRI-NF session.

Neurofeedback runs

Since eight out of 10 subjects were able to self-modulate their own functional connectivity between the NF target in at least one of the neurofeedback runs, these results seem to suggest that this motor imagery paradigm is feasible. Considering 30 NF runs, nine of them were successful, i.e. the subjects were able to self-modulate functional connectivity between bilateral PMC as proposed.

In terms of variation of BOLD signal in the **i.Increase** condition, subjects were able to increase and consequently decrease bilateral premotor activity within the 20 point block. However, **ii.Decrease** correlation values, throughout all ten subjects were relatively far from the low values intended. These high correlation values made more difficult in various runs to have a correct differentiation between conditions.

High condition ii.Decrease correlation values

From the alternatives stated that could be the reason of higher correlation values in condition **i.Increase**, through inspecting the ERA of the correlations in chosen NF runs, it is visible that in some cases, correlation values are indeed elevated and even increasing during **i.Increase** condition blocks,

but for some reason **ii.Decrease** condition blocks had a higher correlation values. This means that even in runs that are not considered to be successful, subjects still successfully increase their own functional connectivity between bilateral premotor in condition **i.Increase**.

One possible reason is due to hemodynamic delay plus the delay due to the calculation of the sliding window Pearson Correlation Coefficient, the feedback presented to the subject in the beginning of each run has information about the previous block. This happens during the first several seconds of each block. This could cause strategy abandonments and confounds. This effect can be more frustrating in conditions that have no strict strategy, just like in the condition **ii.Decrease** There is also an individual lag, i.e., each subject has its own hemodynamic response that could be different even for each run. It is possible, for some subjects such lag that that in fact the correlations measured in the condition **ii.Decrease** are actually related with the mental activation of the task of the previous **i.Increase** condition.

Another possible explanation for high values of correlation in condition **ii.Decrease** is the lack of strict strategy that can cause loss of focus, confounds in strategy and make the subjects more prone to distraction with the thermometer, increasing the sensory activation of the PMC and raising eye movements that also activate the premotor areas. This suggests a hypothesis of a moving visual cue for a baseline or a down regulation condition not being ideal in a PMC activation experiment, although confirmation is required. The data results, as well as the debriefing shows that subjects were more able to self-modulate their functional connectivity in the condition where there was a stricter strategy.

Sliding window Pearson Correlation as measure of FC

Other important variable is the measurement of functional connectivity, using the eight point sliding window Pearson Correlation Coefficient. This approach is also used in the work of Spetter et al. (2017). The interval of points from which one measure is done was chosen beforehand, as good theoretical compromise between the block size and the number of measures. The window size was offline tested after the first pilot and was assumed as having a good balance capturing the differences between conditions and to ensure that there is no rapid variations in the feedback presented. However, more information is required to conclude that this is the optimal approach. With fewer point, the decrease the delay of the feedback would be an advantage. However it could possibly increase the

rapid variation of feedback within a block, possibly causing a sense of frustration on the subjects. Wider sliding windows would present a more stable feedback, but a lot of task-related valid information would also be lost (Zilverstand et al., 2014).

So a methodological approach to determine the best window size is required for protocol optimization.

Debriefing analysis

The feedback from the subject is one important factor to evaluate the success of a Neurofeedback experimental protocol. Since the main objective of NF-training is that a person is able to learn to volitionally control a specific brain region or network with his own mind, the experiment has to be well designed so that participants do not feel frustrated or discouraged, especially when performing the reference task. The main findings for the debriefing were that sense of self-modulation was less present in the down-regulation part of the experiment. This suggests, in further studies, not to present the feedback during decrease functional connectivity as in the work of Ruiz et al. (2014) and Spetter et al. (2017), or at least, optimize the feedback calculation and presentation in this condition **ii.Decrease**.

However, most of the subjects felt in control in the up-regulation of the feedback, suggesting once again the feasibility of this fc-based rt-fMRI-NF experiment. This means that there was a successful up-regulation between bilateral PMC achieved with only one NF-training session, instead of the few sessions reported by Ruiz et al. (2014).

In the NF runs, even though a reference task is given, is done in such way that allows to each participant to adapt its strategy, according to the real time results that they have access to. However, NF is essentially a skill, therefore instructions and references are to be given in order to better perfect it. Not doing it so, there is a risk of the entire rt-fMRI-NF session becoming a search for a suitable strategy, losing statistical power and the possible NF-training effect.

In the debriefing, for the increase connectivity block, subjects described as best resulting tasks: imagining playing drums, opening and closing both hands, finger tapping sequences, playing

the piano, clapping, symmetric arm movement. For the decrease connectivity block, subjects described as best resulting tasks: mathematical calculation, N-back tasks, imagining chores, imagining colors.

Training and Transfer runs

In terms of Training and Transfer, worst results are reported in the Transfer run. This could be because of NF training did not work, comparing Pre and Post, but it is more likely that these bad results in Transfer, (as well as in some Neurofeedback run 3 results) are caused by tiredness, since this experimental protocol is quite demanding mentally and half of the subjects reported mental fatigue in the latter stages of the experiment.

Additionally, significant differences in the distributions of the correlations between Training and Transfer were not expected since most of the NF-training experiments take place with a time window period of days and weeks, with multiple sessions before the effect of the learning skill is expected to be noted (Sulzer et al., 2013).

Nevertheless, it was still reported an improvement in the decreasing of correlation values in the **ii.Decrease** conditions or the increasing of correlation values in the **i.Increase** condition, in three different runs. This shows the possibility of a NF- training effect in functional connectivity self-regulation if this session was to repeat itself several times, comparing to a “sham” feedback control group, as in previous NF experiments (Sulzer et al., 2013).

Conclusion

The main goal of this work was to develop and optimize a framework for enabling self-modulation of interhemispheric functional connectivity between bilateral premotor cortices in an rt-fMRI-NF experiment using a motor imagery paradigm.

A key finding in this project was the optimization of correlation values in activation condition blocks, volitionally variating the BOLD signal. This was possible using the strategy of gradually changing the frequency of imagined movements.

Accounting for pilot studies and the 10 subject acquisitions, the results show a promising outcome since eight out of 10 managed to self-modulate their own functional connectivity with continuous visual feedback. This is confirmed by the subjects feedback, since the majority claimed that they could up-regulate functional connectivity between bilateral PMC. Other important result was the improvement, in three runs, of the correlation between activations, comparing runs before and after NF runs. This suggests a possible NF- training effect in functional connectivity self-modulation.

Given the novelty of the technique these results also open up a variety of questions about the underlying processes inherent to mean BOLD activity of the rPMC and lPMC. Also, the cause of high correlation values in down-regulation conditions needs a further study in order to optimize protocol whether by defining a stricter reference task or changing the type of feedback representation and calculation. A future study could be performed relating the data results with the feedback given by the participants in terms of used tasks for further understanding functional connectivity between bilateral PMC.

Adding to future studies, one can also consider that effective connectivity studies should be done in order to find a possible effect in NF training in motor network. With an optimized protocol to maximize differences of correlations between conditions, functional connectivity-based rt-fMRI-NF could be a possible therapeutical tool in clinical trials in diseases related with interhemispheric connectivity impairment such as Alzheimer’s, Parkinson's and particularly in motor cortex, stroke.

References

Abdulkader, Sarah N., Ayman Atia, and Mostafa-Sami M. Mostafa. 2015. “Brain Computer Interfacing: Applications and Challenges.” Egyptian Informatics Journal 16 (2): 213–30.

Aramaki, Y., M. Honda, and N. Sadato. 2006. “Suppression of the Non-Dominant Motor Cortex during Bimanual Symmetric Finger Movement: A Functional Magnetic Resonance Imaging Study.” Neuroscience 141 (4): 2147–53.

Arthurs, Owen J., and Simon Boniface. 2002. “How Well Do We Understand the Neural Origins of the fMRI BOLD Signal?” Trends in Neurosciences 25 (1): 27–31.

Barron, Helen C., Mona M. Garvert, and Timothy E. J. Behrens. 2016. “Repetition Suppression: A Means to Index Neural Representations Using BOLD?” Philosophical Transactions of the Royal Society of London. Series B, Biological Sciences 371 (1705). doi:10.1098/rstb.2015.0355.

Berman, Brian D., Silvina G. Horovitz, Gaurav Venkataraman, and Mark Hallett. 2012. “Self-Modulation of Primary Motor Cortex Activity with Motor and Motor Imagery Tasks Using Real-Time fMRI-Based Neurofeedback.” NeuroImage 59 (2): 917–25.

Biswal, B., F. Z. Yetkin, V. M. Haughton, and J. S. Hyde. 1995. “Functional Connectivity in the Motor Cortex of Resting Human Brain Using Echo-Planar MRI.” Magnetic Resonance in Medicine: Official Journal of the Society of Magnetic Resonance in Medicine / Society of Magnetic Resonance in Medicine 34 (4): 537–41.

Bullmore, Ed. 2012. “The Future of Functional MRI in Clinical Medicine.” NeuroImage 62 (2): 1267–71.

Caria, Andrea, Ranganatha Sitaram, Ralf Veit, Chiara Begliomini, and Niels Birbaumer. 2010. “Volitional Control of Anterior Insula Activity Modulates the Response to Aversive Stimuli. A Real-Time Functional Magnetic Resonance Imaging Study.” Biological Psychiatry 68 (5): 425–32.

Coben, Robert, Michael Linden, and Thomas E. Myers. 2010. “Neurofeedback for Autistic Spectrum Disorder: A Review of the Literature.” Applied Psychophysiology and Biofeedback 35 (1): 83–105.

Cox, Robert W., Andrzej Jesmanowicz, and James S. Hyde. 1995. “Real-Time Functional Magnetic Resonance Imaging.” Magnetic Resonance in Medicine: Official Journal of the Society of Magnetic Resonance in Medicine / Society of Magnetic Resonance in Medicine 33 (2): 230–36.

Decety, J. 1996. “The Neurophysiological Basis of Motor Imagery.” Behavioural Brain Research 77 (1-2): 45–52.

Dechent, P., Merboldt, K.-D., & Frahm, J. (2004). Is the human primary motor cortex involved in motor imagery? Brain Research. Cognitive Brain Research, 19(2), 138–144. doi:10.1016/j.cogbrainres.2003.11.012

Eiji Hoshi, Jun Tanji, Distinctions between dorsal and ventral premotor areas: anatomical connectivity and functional properties, Current Opinion in Neurobiology, Volume 17, Issue 2, April 2007, Pages 234-242, ISSN 0959-4388, http://dx.doi.org/10.1016/j.conb.2007.02.003. (http://www.sciencedirect.com/science/article/pii/S095943880700027X).

Faro, Scott H., and Feroze B. Mohamed. 2010. BOLD fMRI: A Guide to Functional Imaging for Neuroscientists. Springer Science & Business Media.

Friston, Karl J. 2011. "Functional and Effective Connectivity: A Review." Brain Connectivity 1 (1): 13–36.

Gerardin, E., Sirigu, A., Lehéricy S., Poline, JB., Gaymard, B., Marsault, C., Agid, Y., Le Bihan, D (2000). "Partially overlapping neural networks for real and imagined hand movements" Cereb. Cortex, 10 (11), 1093-1104, doi: 10.1093/cercor/10.11.10937

Gerstein, G. L., and D. H. Perkel. 1969. "Simultaneously Recorded Trains of Action Potentials: Analysis and Functional Interpretation." Science 164 (3881): 828–30.

Grefkes, Christian, Simon B. Eickhoff, Dennis A. Nowak, Manuel Dafotakis, and Gereon R. Fink. 2008. "Dynamic Intra- and Interhemispheric Interactions during Unilateral and Bilateral Hand Movements Assessed with fMRI and DCM." NeuroImage 41 (4): 1382–94.

Guillot, A., Di Rienzo, F., Collet, C. (2014). The neurofunctional architecture of motor imagery. "Functional magnetic resonance imaging", 1, 16, http://dx.doi.org/10.5772/30961.

Hanakawa, T., Immisch, I., Toma, K., Dimyan, M. A., Van Gelderen, P., & Hallett, M. (2003). Functional properties of brain areas associated with motor execution and imagery. Journal of Neurophysiology, 89(2), 989-1002, doi: 10.1152/jn.00132.2002

Heuvel, Martijn P. van den, and Hilleke E. Hulshoff Pol. 2010. "Exploring the Brain Network: A Review on Resting-State fMRI Functional Connectivity." European Neuropsychopharmacology: The Journal of the European College of Neuropsychopharmacology 20 (8): 519–34.

Hui, M, Zhang, H., Ge, R., Yao, L., & Long, Z. (2014). Modulation of functional network with real-time fMRI feedback training of right premotor cortex activity. Neuropsychologia, 62, 111–123. doi:10.1016/j.neuropsychologia.2014.07.012

Jeannerod, M. 1994. "The Representing Brain: Neural Correlates of Motor Intention and Imagery." The Behavioral and Brain Sciences 17 (02): 187.

Josephs, O., and R. N. Henson. 1999. "Event-Related Functional Magnetic Resonance Imaging: Modelling, Inference and Optimization." Philosophical Transactions of the Royal Society of London. Series B, Biological Sciences 354 (1387): 1215–28.

Kim, J., Lee, J., Jo, H. J., Kim, S. H., Lee, J. H., Tae, S., Saad, Z. S. (2010). Defining functional SMA and pre-SMA subregions in human MFC using resting state fMRI: functional connectivity-based parcellation method. NeuroImage, 49(3), 1–22. doi:10.1016/j.neuroimage.2009.10.016.Defining

Koush, Yury, Maria Joao Rosa, Fabien Robineau, Klaartje Heinen, Sebastian W Rieger, Nikolaus Weiskopf, Patrik Vuilleumier, Dimitri Van De Ville, and Frank Scharnowski. 2013. "Connectivity-

Based Neurofeedback: Dynamic Causal Modeling for Real-Time fMRI." NeuroImage 81 (November): 422–30.

Lacourse, Michael; Orr, Elizabeth; Cramer, Steven; Cohen, Michael (2005) .Brain activation during execution and motor imagery of novel and skilled sequential hand movements. NeuroImage, 27, 505-519, doi:10.1016/j.neuroimage.2005.04.025

Liuzzi, G., Hörniß, V., Zimerman, M., Gerloff, C., & Hummel, F. C. (2011). Coordination of uncoupled bimanual movements by strictly timed interhemispheric connectivity. The Journal of Neuroscience, 31(25), 9111-9117, DOI: 10.1523/JNEUROSCI.0046-11.2011

Logothetis, Nikos K., and Brian A. Wandell. 2004. "Interpreting the BOLD Signal." Annual Review of Physiology 66 (1): 735–69.

Matsumoto, Riki, Dileep R. Nair, Eric LaPresto, William Bingaman, Hiroshi Shibasaki, and Hans O. Lüders. 2007. "Functional Connectivity in Human Cortical Motor System: A Cortico-Cortical Evoked Potential Study." Brain: A Journal of Neurology 130 (Pt 1): 181– 97.

Mendes, Pedro Alexandre, Daniel A. Marinho, João Duarte Petrica, Paulo Silveira, Diogo Monteiro, and Luis Cid. 2016. "Tradução E Validação Do Movement Imagery Questionnaire – 3 (MIQ - 3) Com Atletas Portugueses." Motricidade 12 (1): 149.

Minshew, Nancy J., and Timothy A. Keller. 2010. "The Nature of Brain Dysfunction in Autism: Functional Brain Imaging Studies." Current Opinion in Neurology 23 (2): 124–30.

Mulert, Christoph, and Martha E. Shenton. 2014. MRI in Psychiatry. Springer.

Munzert, Jörn, Britta Lorey, and Karen Zentgraf. 2009. "Cognitive Motor Processes: The Role of Motor Imagery in the Study of Motor Representations." Brain Research Reviews 60 (2): 306–26.

New, Anneliese B., Donald A. Robin, Amy L. Parkinson, Joseph R. Duffy, Malcom R. McNeil, Olivier Piguet, Michael Hornberger, Cathy J. Price, Simon B. Eickhoff, and Kirrie J. Ballard. 2015. "Altered Resting-State Network Connectivity in Stroke Patients with and without Apraxia of Speech." NeuroImage. Clinical 8 (March): 429–39.

Ogawa, S., Lee, T. M., Kay, A. R., & Tank, D. W. (1990). Brain magnetic resonance imaging with contrast dependent on blood oxygenation. Proceedings of the National Academy of Sciences, 87(24), 9868–9872.

Piokenhain, L. 1984. "Chapter Vb Towards a Holistic Conception of Movement Control." In Advances in Psychology, 505–28.

Poston, Kathleen L., and David Eidelberg. 2012. "Functional Brain Networks and Abnormal Connectivity in the Movement Disorders." NeuroImage 62 (4): 2261–70.

Purves D, Augustine GJ, Fitzpatrick D, et al., editors. Neuroscience. 2nd edition. Sunderland (MA): Sinauer Associates; 2001. The Premotor Cortex.Available from: http://www.ncbi.nlm.nih.gov/books/NBK10796/

Qing Gao, Xujun Duan, Huafu Chen, (2011). Evaluation of effective connectivity of motor areas during motor imagery and execution using conditional Granger causality. NeuroImage, 54, 1280–1288, doi:10.1016/j.neuroimage.2010.08.071

Rao, S. M., P. A. Bandettini, J. R. Binder, J. A. Bobholz, T. A. Hammeke, E. A. Stein, and J. S. Hyde. 1996. “Relationship between Finger Movement Rate and Functional Magnetic Resonance Signal Change in Human Primary Motor Cortex.” Journal of Cerebral Blood Flow and Metabolism: Official Journal of the International Society of Cerebral Blood Flow and Metabolism 16 (6): 1250–54.

Ravenel, James. 2003. “The Essential Physics of Medical Imaging, 2nd Ed.” American Journal of Roentgenology 180 (3): 596–596.

Rizzolatti, G., G. Luppino, and M. Matelli. 1998. “The Organization of the Cortical Motor System: New Concepts.” Electroencephalography and Clinical Neurophysiology 106 (4): 283–96.

Rota, Giuseppina, Ranganatha Sitaram, Ralf Veit, Michael Erb, Nikolaus Weiskopf, Grzegorz Dogil, and Niels Birbaumer. 2009. “Self-Regulation of Regional Cortical Activity Using Real-Time fMRI: The Right Inferior Frontal Gyrus and Linguistic Processing.” Human Brain Mapping 30 (5): 1605–14.

Ruiz, Sergio, Korhan Buyukturkoglu, Mohit Rana, Niels Birbaumer, and Ranganatha Sitaram. 2014. “Real-Time fMRI Brain Computer Interfaces: Self-Regulation of Single Brain Regions to Networks.” Biological Psychology 95 (January): 4–20.

Siero, Jeroen C. W., Alex Bhogal, and J. Martijn Jansma. 2013. “Blood Oxygenation Level-dependent/Functional Magnetic Resonance Imaging: Underpinnings, Practice, and Perspectives.” PET Clinics 8 (3): 329–44.

Sitaram, Ranganatha, Sangkyun Lee, Sergio Ruiz, and Niels Birbaumer. 2011. “Real-Time Regulation and Detection of Brain States from fMRI Signals.” In Neurofeedback and Neuromodulation Techniques and Applications, 227–438.

Sitaram, Ranganatha, Tomas Ros, Luke Stoeckel, Sven Haller, Frank Scharnowski, Jarrod Lewis-Peacock, Nikolaus Weiskopf, et al. 2017. “Closed-Loop Brain Training: The Science of Neurofeedback.” Nature Reviews. Neuroscience 18 (2): 86–100.

Smith, Stephen M., Karla L. Miller, Gholamreza Salimi-Khorshidi, Matthew Webster, Christian F. Beckmann, Thomas E. Nichols, Joseph D. Ramsey, and Mark W. Woolrich. 2011. “Network Modelling Methods for FMRI.” NeuroImage 54 (2): 875–91.

Solodkin, A., Hlustik, P., Chen, E. E., & Small, S. L. (2004). Fine modulation in network activation during motor execution and motor imagery. Cerebral Cortex, 14(11), 1246–1255. doi:10.1093/cercor/bhh086

Spetter, Maartje S., Rahim Malekshahi, Niels Birbaumer, Michael Lührs, Albert H. van der Veer, Klaus Scheffler, Sophia Spuckti, Hubert Preissl, Ralf Veit, and Manfred Hallschmid. 2017. “Volitional Regulation of Brain Responses to Food Stimuli in Overweight and Obese Subjects: A Real-Time fMRI Feedback Study.” Appetite 112 (January): 188–95.

Stephan, Klaas E., John C. Marshall, Will D. Penny, Karl J. Friston, and Gereon R. Fink. 2007. “Interhemispheric Integration of Visual Processing during Task-Driven Lateralization.” The Journal of Neuroscience: The Official Journal of the Society for Neuroscience 27 (13): 3512–22.

Stephan, Klaas E., Torsten Baldeweg, and Karl J. Friston. 2006. “Synaptic Plasticity and Dysconnection in Schizophrenia.” Biological Psychiatry 59 (10): 929–39.

Sulzer, J., S. Haller, F. Scharnowski, N. Weiskopf, N. Birbaumer, M. L. Blefari, A. B. Bruehl, et al. 2013. “Real-Time fMRI Neurofeedback: Progress and Challenges.” NeuroImage 76 (August): 386–99.

Sun, Y., Wei, W., Luo, Z., Gan, H., & Hu, X. (2016). Improving motor imagery practice with synchronous action observation in stroke patients. Topics in stroke rehabilitation, 1-9. DOI:10.1080/10749357.2016.1141472

Swinnen, Stephan P., and Nicole Wenderoth. 2004. “Two Hands, One Brain: Cognitive Neuroscience of Bimanual Skill.” Trends in Cognitive Sciences 8 (1): 18–25.

Talairach, Jean, and Pierre Tournoux. 1988. Co-Planar Stereotaxic Atlas of the Human Brain: 3-Dimensional Proportional System: An Approach to Cerebral Imaging. George Thieme Verlag.

Weiskopf, Nikolaus, Frank Scharnowski, Ralf Veit, Rainer Goebel, Niels Birbaumer, and Klaus Mathiak. 2004. “Self-Regulation of Local Brain Activity Using Real-Time Functional Magnetic Resonance Imaging (fMRI).” Journal of Physiology, Paris 98 (4-6): 357–73.

Weiskopf, Nikolaus, Klaus Mathiak, Simon W. Bock, Frank Scharnowski, Ralf Veit, Wolfgang Grodd, Rainer Goebel, and Niels Birbaumer. 2004. “Principles of a Brain-Computer Interface (BCI) Based on Real-Time Functional Magnetic Resonance Imaging (fMRI).” IEEE Transactions on Bio-Medical Engineering 51 (6): 966–70.

Weiskopf, Nikolaus. 2012. “Real-Time fMRI and Its Application to Neurofeedback.” NeuroImage 62 (2): 682–92.

Wolpert, D. M., & Ghahramani, Z. (2000). Computational principles of movement neuroscience. nature neuroscience, 3, 1212–1217.

Xie, F., Xu, L., Long, Z., Yao, L., & Wu, X. 2015. Functional connectivity alteration after real-time fMRI motor imagery training through self-regulation of activities of the right premotor cortex. BMC neuroscience, 16 (1), 1, doi: 10.1186/s12868-015-0167-1

Zarahn, E., G. K. Aguirre, and M. D’Esposito. 1997. “Empirical Analyses of BOLD fMRI Statistics.” NeuroImage 5 (3): 179–97.

Zhang, H., Xu, L., Wang, S., Xie, B., Guo, J., Long, Z., & Yao, L. (2011). Behavioral improvements and brain functional alterations by motor imagery training. Brain research, 1407, 38-46, doi:10.1016/j.brainres.2011.06.038

Zhang, Hui, Jie Tian, and Zonglei Zhen. 2007. “Direct Measure of Local Region Functional Connectivity by Multivariate Correlation Technique.” Conference Proceedings: ... Annual International Conference of the IEEE Engineering in Medicine and Biology Society. IEEE Engineering in Medicine and Biology Society. Conference 2007: 5231–34.

Zilverstand, Anna, Bettina Sorger, Jan Zimmermann, Amanda Kaas, and Rainer Goebel. 2014. "Windowed Correlation: A Suitable Tool for Providing Dynamic fMRI-Based Functional Connectivity Neurofeedback on Task Difficulty." PloS One 9 (1): e85929.

Online References

All online references were last accessed on the 16th of February of 2017

[1]Becker, Benjamin "Fronto-limbic Functional Connectivity Via Real-time fMRI Neurofeedback" https://clinicaltrials.gov/ct2/show/NCT02692196

[2]http://www.brainvoyager.com/bvqx/doc/UsersGuide/StatisticalAnalysis/TheGeneralLinearModel.html

[3]http://download.brainvoyager.com/tbv/TBVUsersGuide/Setup/SetupForNeurofeedback.html

[4]http://www.brainvoyager.com/bvqx/doc/UsersGuide/Preprocessing/SliceScanTimeCorrection.html

[5]http://www.brainvoyager.com/bvqx/doc/UsersGuide/Preprocessing/MotionDetectionAndCorrection.html

[6]http://www.brainvoyager.com/bvqx/doc/UsersGuide/Preprocessing/TemporalHighPassFiltering.html

[7]http://www.brainvoyager.com/bvqx/doc/UsersGuide/Coregistration/CoregistrationOfFunctionalAndAnatomicalDataSets.html

[8]http://www.brainvoyager.com/bvqx/doc/UsersGuide/BrainNormalization/ManualACPCAndTalairachTransformation.html

[9]http://www.brainvoyager.com/bvqx/doc/UsersGuide/VTCCreation/FromFMR-STCsToVTCsInTalairachSpace.html

[10]http://www.brainvoyager.com/bvqx/doc/UsersGuide/StatisticalAnalysis/SingleSubjectAnalysis/SingleSubjectGLMAnalysis.html

[11]http://www.brainvoyager.com/bvqx/doc/UsersGuide/StatisticalAnalysis/RandomEffectsAnalysis/RandomEffectsGroupAnalysis.html

Annex I. MIQ -3 Results

			MIQ - 3 Motor Imagery Questionnaire											
Subject	**Age**	**Gender**	**1**	**2**	**3**	**4**	**5**	**6**	**7**	**8**	**9**	**10**	**11**	**12**
Subject 1	27	M	6	6	4	4	6	5	4	5	4	4	6	5
Subject 2	28	M	7	6	7	7	7	7	7	7	7	5	7	7
Subject 3	28	M	7	5	6	6	7	4	7	5	5	6	6	4
Subject 4	23	M	6	5	6	6	5	4	6	6	5	6	6	5
Subject 5	33	F	5	6	6	5	6	6	5	5	6	5	6	6
Subject 6	23	M	5	4	6	4	6	6	5	4	7	5	6	6
Subject 7	29	F	7	6	7	7	6	7	7	7	7	7	7	7
Subject 8	24	M	6	5	5	6	6	5	5	6	5	6	6	5
Subject 9	27	F	4	6	6	5	5	6	5	6	6	5	6	6
Subject 10	23	M	5	6	6	4	5	6	5	6	5	4	6	5

Annex II. Debriefing

Aquisições – Motor Imagery Paradigm

Nome: Idade: Data:

1. Como se sentiu durante a sessão inteira deste teste piloto?

_____
_____
_____
_____

2. Sentiu dificuldades na tarefa motora e mental da *run* do "Localizer"?

_____
_____

3. Que estratégias mentais funcionaram melhor nas *runs* de Neurofeedback?

_____
_____
_____
_____

4. Que estratégias mentais funcionaram pior nas *runs* de Neurofeedback?

_____
_____
_____
_____

5. Sentiu que conseguiu modular os valores do termómetro da maneira pretendida?

_____
_____
_____

6. Outros comentários/sugestões acerca do Protocolo Experimental?

_____
_____
_____
_____

Subject	Question 1
Subject 1	Senti-me bem, já estou habituado a fazer fMRI.
Subject 2	Bem, mas mais cansado para o fim.
Subject 3	Bem, sem desconforto.
Subject 4	Bem, um pouco cansado no fim, o que levou a mente a divagar.
Subject 5	Bem, mas cansada nas duas últimas runs.
Subject 6	Bem
Subject 7	Mais ou menos, ligeiramente frustrada.
Subject 8	Algum nervosismo no inicio.
Subject 9	Normal, com sonolência.
Subject 10	Cansado para o final.

Subject	Question 2
Subject 1	Não
Subject 2	Não
Subject 3	Não
Subject 4	Não
Subject 5	Não
Subject 6	Não - a instrução deveria aparecer durante mais tempo.
Subject 7	Não
Subject 8	Não
Subject 9	Não
Subject 10	Não

Subject	Question 3
Subject 1	Imaginar cócegas a outra pessoa, em bursts intermitentes, parando depois do beep a meio do bloco.
Subject 2	Imaginar o processo de tocar bateria como um todo.
Subject 3	Movimentos coordenado de braços.
Subject 4	Movimentos mais gerais. Movimentos menos localizados. Movimentos mais usados em tarefas comuns, menos abstratos.
Subject 5	Abrir e fechar mãos em Increased e imaginar caras de pessoas ou cores ou em coisas que tenho para fazer (trabalho, jantar...) na Decreased.
Subject 6	Imaginação somente de carregar nos botões da ressonância. Carregar em 4 teclas de um piano.

Subject 7	Imaginação da sequência do Localizer com ambas as mãos em simultâneo.
Subject 8	Multiplicações e pensar em nomes de cores em inglês durante Decreased.
Subject 9	Imaginar bater palmas.
Subject 10	Increased - movimentos dessincronizado/alternado ; bimanual simétrico - fase de preparação para salto de cabeça para a piscina. Decreased - N-back e cálculos.

Subject	**Question 4**
Subject 1	Variação de frequência não funcionou muito bem.
Subject 2	Quando estava a imaginar o processo desconstruído.
Subject 3	Quando imaginei um movimento descoordenado aleatório.
Subject 4	Usar movimentos abstratos.
Subject 5	Focar nas barras do termómetro.
Subject 6	Movimento de dedos de ambas as mãos, diferente.
Subject 7	Imaginação de outras tarefas motoras.
Subject 8	Somas e operações matemáticas simples na Decrease.
Subject 9	Fechar os olhos durante o Decrease.
Subject 10	Decreased - não pensar em nada; Increased - não conseguia imaginar outra coisa, distração com o termómetro.

Subject	**Question 5**
Subject 1	Não funcionou muito bem.
Subject 2	Sim, em geral.
Subject 3	No Increased consegui obter correspondência na maior parte das vezes. Na Decrease nem sempre.
Subject 4	Algumas vezes, sendo mais fácil no fim de cada run. Decreased no início parece mais difícil.
Subject 5	Sim, embora não sempre.
Subject 6	Nem por isso, e por vezes parece atrasado em relação ao esperado.
Subject 7	Apenas a parte inicial de 1 ou 2 runs.
Subject 8	Mais dificuldade nos blocos de Decreased.
Subject 9	Sim, significativamente.
Subject 10	Sim, mas não na totalidade do bloco.

Subject	Question 6
Subject 1	Feedback contínuo (curva) em vez de termómetro talvez fosse interessante.
Subject 2	O termómetro pode induzir em erro devido ao delay.
Subject 3	-
Subject 4	Mostrar BOLD de cada premotor poderia ajudar.
Subject 5	-
Subject 6	-
Subject 7	Instrução para Decreased deveria ser movimento descordenado.
Subject 8	Fazer um primeiro run de teste, fora da ressonância mas visualizando o que se vê no ecrã lá dentro.
Subject 9	-
Subject 10	-

Annex III. Normalization Tests

Table 1. Normality distribution for the First Pilot, using Lilliefors test with the null hypothesis that the correlation in each run comes from a distribution in the normal family, against the alternative that it does not come from such a distribution with 0.05 significance level.

	Bimanual			Unimanual			Baseline		
Run \ Condition	**p**	**h**	**stats**	**p**	**h**	**stats**	**p**	**h**	**stats**
Training	4,65E-02	1	1,00E-01	9,10E-03	1	1,17E-01	1,00E-03	1	1,42E-01
NF run 1	1,00E-03	1	1,93E-01	2,33E-01	0	7,99E-02	5,47E-03	1	8,15E-02
NF run 2	7,65E-02	0	9,43E-02	4,78E-02	1	9,97E-02	1,00E-03	1	1,16E-01
NF run 3	1,00E-03	1	1,83E-01	1,06E-02	1	1,15E-01	1,46E-03	1	8,90E-02
Transfer	4,01E-03	1	1,24E-01	5,00E-01	0	6,64E-02	1,00E-03	1	1,07E-01

Table 2. Normality distribution for the Second Pilot, using Lilliefors test with the null hypothesis that the correlation in each run follows a normal distribution, against the alternative that it does not with 0.05 significance level.

	Bimanual			Unimanual			Baseline		
Run \ Condition	**p**	**h**	**stats**	**p**	**h**	**stats**	**p**	**h**	**stats**
Training	1,31E-03	1	1,33E-01	2,77E-01	0	7,72E-02	5,77E-02	0	6,57E-02
NF run 1	8,95E-03	1	1,17E-01	1,34E-01	0	8,74E-02	4,99E-03	1	8,20E-02
NF run 2	1,66E-01	0	8,45E-02	1,55E-01	0	8,55E-02	2,67E-01	0	5,24E-02
NF run 3	7,89E-02	0	9,40E-02	2,80E-03	1	1,27E-01	5,15E-02	0	6,65E-02
Transfer	5,00E-01	0	5,44E-02	1,48E-01	0	8,62E-02	1,25E-03	1	8,99E-02

Table 3. Normality distribution for the Third Pilot, using Lilliefors test with the null hypothesis that the correlation in each run comes from a distribution in the normal family, against the alternative that it does not come from such a distribution with 0.05 significance level.

	Bimanual			Unimanual			Baseline		
Run \ Condition	**p**	**h**	**stats**	**p**	**h**	**stats**	**p**	**h**	**stats**
Training	1,36E-03	1	1,33E-01	1,00E-03	1	1,38E-01	7,88E-03	1	7,93E-02
NF run 1	1,00E-03	1	1,42E-01	8,70E-02	0	9,28E-02	1,00E-03	1	1,51E-01
NF run 2	1,00E-03	1	1,47E-01	6,04E-03	1	1,20E-01	9,13E-02	0	6,21E-02
NF run 3	5,88E-03	1	1,20E-01	2,12E-01	0	8,12E-02	1,00E-03	1	9,39E-02
Transfer	4,68E-02	1	9,99E-02	1,38E-03	1	1,33E-01	1,00E-03	1	9,52E-02

Table 4. Normality distribution for the Fourth Pilot, using Lilliefors test with the null hypothesis that the correlation in each run comes from a distribution in the normal family, against the alternative that it does not come from such a distribution with 0.05 significance level.

	Bimanual			Unimanual			Baseline		
Run \ Condition	**p**	**h**	**stats**	**p**	**h**	**stats**	**p**	**h**	**stats**
Training	1,53E-02	1	1,12E-01	1,00E-03	1	1,41E-01	1,01E-01	0	6,12E-02
NF run 1	1,00E-03	1	1,36E-01	4,97E-02	1	9,93E-02	1,16E-03	1	9,03E-02
NF run 2	1,00E-03	1	1,77E-01	1,00E-03	1	1,48E-01	1,76E-03	1	8,80E-02
NF run 3	2,68E-01	0	7,77E-02	2,89E-02	1	1,05E-01	1,00E-03	1	1,38E-01
Transfer	1,00E-03	1	1,38E-01	1,00E-03	1	1,54E-01	1,00E-03	1	1,09E-01